Materials Today Energy 23 (2022) 100900

Contents lists available at ScienceDirect

Materials Today Energy

journal homepage: www.journals.elsevier.com/materials-today-energy/

Self-powered and wearable biosensors for healthcare

Xiaolong Zeng [a, b, e], Ruiheng Peng [a, e], Zhiyong Fan [c, d, **], Yuanjing Lin [a, b, *]

[a] School of Microelectronics, Southern University of Science and Technology, Shenzhen 518055, China
[b] Engineering Research Center of Integrated Circuits for Next-Generation Communications, Ministry of Education, Southern University of Science and Technology, Shenzhen 518055, China
[c] Department of Electronic & Computer Engineering, The Hong Kong University of Science and Technology, Clear Water Bay, Kowloon, Hong Kong Special Administrative Region
[d] HKUST-Shenzhen Research Institute, No. 9 Yuexing First RD, South Area, Hi-tech Park, Nanshan, Shenzhen 518057, China

ARTICLE INFO

Article history:
Received 15 September 2021
Received in revised form
2 November 2021
Accepted 8 November 2021
Available online 12 November 2021

Keywords:
Electrochemical biosensors
Self-powered systems
Wearable devices
Power management
Health-care monitoring

ABSTRACT

The integration of energy collection and storage modules with wearable biosensors can drive the entire biosensing system to obtain human health information in a self-powered fashion, without external charging. Research advances in the development of wearable devices have demonstrated their promising applications for body status monitoring. Herein, an overview of electrochemical biosensors and their integration into self-powered and wearable devices for health-care applications is provided. The sensing mechanisms of the commonly adopted electrochemical biosensors are first summarized, followed by the research progress on self-powered biosensing systems based on various energy harvesting methods. To further understand the effective utilization of energy from different harvesting and conversion methods with desired power output, power management strategies to ensure stable and continuous energy supply are introduced. Finally, the key challenges that currently limit the practical applications of self-powered devices are discussed, along with the prospects of monitoring our health status with wearable biosensors in a convenient and personalized manner.

1. Introduction

Wearable biosensors can detect physical signals such as heart rate and human activities, as well as physiological information in various body fluids that can be extracted in a minimal/non-invasive manner. A variety of biosensors, such as glucose sensors, lactate sensors, uric acid (UA) sensors, has been successfully integrated into wearable platforms such as watches [1], glass [2], and mouthguards [3–6]. They provide the merits of convenience and continuous health monitoring with low infection risks and have the potential to serve as a supplement to traditional test methods such as blood tests [7–11]. With the popularity of mobile devices, mobile healthcare based on wearable biosensors attracts tremendous interest as one of the most promising technologies to achieve personalized healthcare and release clinical resource pressure [12–14]. The desired form factors of these wearable biosensing electronics include flexibility, lightweight, smart sensing, and data display with long operation duration [15].

To fulfill the above requirements, wearable biosensing systems with self-power capability emerge as one of the most effective strategies. In self-powered devices, the energy required for the device operation is expected to be supported with the energy harvested and converted from the human body and environment, without external charging components. Research efforts in the development of highly efficient energy devices and rational power management strategies play a key role in achieving self-powered and wearable electronic systems with stable power supply and smooth operation. Especially for an integrated system that has electronic devices such as the microcontroller unit and communication module, optimized system working flow and low power consumption are critical. It ensures the system functions of tracking human health information and transmits the data to mobile devices through Bluetooth or near field communication (NFC) modules in a real-time manner [10,16].

In this review, the recent progress of self-powered and wearable biosensors is discussed (Fig. 1). First, biosensors based on different sensing methods are introduced and summarized. Then, various energy harvesting and conversion methods that can be integrated

* Corresponding author.
** Corresponding author.
E-mail addresses: eezfan@ust.hk (Z. Fan), linyj2020@sustech.edu.cn (Y. Lin).
[e] X. Z. and R. P. contributed equally to this review.

https://doi.org/10.1016/j.mtener.2021.100900
2468-6069/

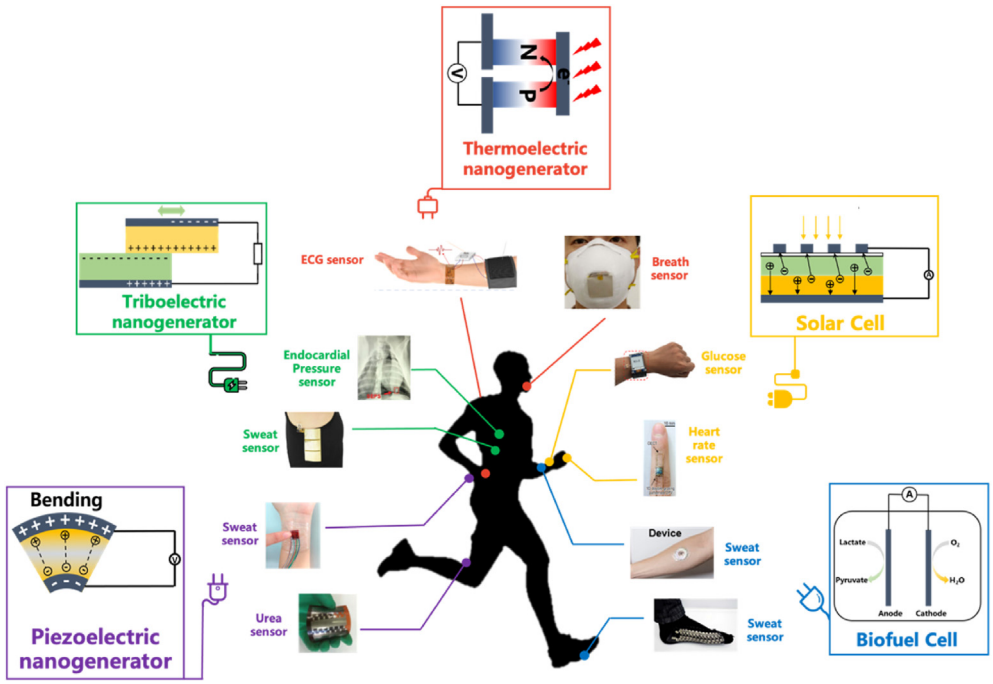

Fig. 1. Representative examples of self-powered wearable biosensors. Clockwise from left: implantable electronic skin based on PENGs [17]. Non-invasive electronic skin based on PENGs [18]. A wireless battery-free wearable sweat sensor based on TENGs [19]. An endocardial pressure sensor based on TENGs [20]. An ECG sensor based on TEGs [21]. A PyNG-based breathing sensor integrated on the N95 mask [22]. A smartwatch used to sweat glucose based on the solar cell [23]. A wearable heart rate sensor based on the solar cell [24]. Battery-free, skin-interfaced microfluidic/electronic systems based on BFCs [25]. Sock-based BFC array [26].

with wearable biosensors are introduced. Besides, the circuit design and rectification methods to realize effective power utilization with energy harvested and converted from the human body and the surrounding environment are highlighted. Further prospects of research on wearable biosensors and self-powered devices are then discussed with consideration of current challenges.

2. Sensing mechanism of electrochemical biosensors

Wearable biosensors have received widespread attention owing to their potential to provide supplementary information for personalized healthcare. The biosensors that can provide molecular-level information to indicate human health states are mostly based on electrochemical mechanisms, including potentiometric, amperometric, differential pulse voltammetric (DPV), and impedance sensing modes. These electrochemical sensors provide high sensitivity, selectivity, low response time, and easy adaptation to wearable devices [11,27]. In this part, the sensing mechanism of the commonly adopted electrochemical biosensors is summarized (Table 1) and presented.

2.1. Potentiometric mode

Potentiometric sensing method is mainly used for ion detection, such as sodium ions (Na^+) and potassium ions (K^+), in which the measurable potential of the sensing electrode changes with the concentration of the target analyte [58]. These sensors normally include a working electrode (WE) with an ion-selective membrane (ISM) and a reference electrode (RE) in a two-electrode system and can be used under near-zero current conditions. The ISM usually contains ionophores, which are fat-soluble, used to bind and carry specific ions along the membrane, and generate a specific potential owing to the induced ion activity. This potential can vary with the concentration of the analyte and is based on the Nernst Eq. (1):

$$E = E^0 + \frac{RT}{nF} In \frac{[RED]}{[OX]} \quad (1)$$

where E is the battery potential, E^0 is the standard potential of the half-reaction, R is the universal gas constant, T is the temperature, n is the number of electrons participating in the half-reaction, F is the Faraday constant, [RED] is the activity of the reducing substance, [OX] is the activity of oxidizing substances. The Nernst factor, RT/F, depends on temperature [27].

Potentiometric sensing test can quickly and real-time reflect the concentration of the analyte, and it has been widely used for sweat ion monitoring. As shown in Fig. 2a–c, Zhai et al. [28] developed a flexible sweat ion sensor based on vertically arranged mushroom-shaped gold nanowires (v-AuNW). By modifying the v-AuNW electrode with polyaniline, Na ionophore X, and a selective membrane based on valinomycin, they can separately detect the pH values, Na^+, and K^+ concentrations with high selectivity, reproducibility, and stability. It is worth noting that even under 30% strain and during the tensile release cycle, its electrochemical performance can remain unchanged. The sensor overcomes the rigidity of traditional solid-state sensors and can be applied to the soft skin of the human body.

The detection scheme and signal processing of the potential sensing method are simple, and it is an ideal option for fixed charged analytes. However, different selective membranes need to be developed for different ions. At the same time, when the analysis ion concentration is too low, interference from other ions could occur.

2.2. Amperometric mode

Amperometry refers to the measurement of current generated by the oxidation-reduction reaction of the analyte on the WE. When applying a constant potential, the electron transfer between the electrode and the analyte during the oxidation or reduction of

Table 1
Electrochemical biosensors in different sensing modes.

Technique	Sensors	Analyte	Recognition element	Detection range	Sensitivity	References
Potentiometry	Sweat	pH	Ionophore	4–8	56.1 mV/pH	[28]
		Na^+		1–100 mM	58.2 mV/decade	
		K^+		1–100 mM	41.5 mV/decade	
	Sweat	Na^+	Ionophore	0.1–100 mM	58.8 mV/log(Na^+)	[29]
		K^+			54.4 mV/log(K^+)	
	Interstitial fluid	K^+	Ionophore	0.1–100 mM	54.5 mV/log(K^+)	[30]
	Sweat	Na^+	ZnO NWs	0.1–100 mM	42.9 mV/log(Na^+)	[31]
		Lactate		0–25 mM	0.94 mV/mM	
	Cu^{2+}	Cu^{2+}	Ionophore	0.25–250 μM	30.7 mV/decade	[32]
Amperometry	Salivary	Glucose	GOx/PB	1.75–10,000 μmol/L	–	[33]
	Perspiration	Glucose	GOx/PB	0.1–25 mM	1.41 μA/mM	[34]
	Glucose	Glucose	GOx/PB	1 μM-20 mM	26.05 μA/(cm^2·mM) (1–100 μM) 10.96 μA/(cm^2·mM) (100 μM–20 mM)	[35]
	Glucose	Glucose	GOx/PB	0–300 μM	216.9 μA/mM	[36]
	Tear	Glucose	GOx/PB	0–50 mg/dL	–	[37]
	Glucose	Glucose	Cu_2O/chitosan	1–4 mM	–	[38]
	Sweat	Lactate	LOx/PB	0–30 mM	19.13 μA/(cm^2 ·mM)	[39]
	Sweat	Lactate	LOx/PB	0–50 mM	36.2 μA/(cm^2·mM)	[40]
	Sweat	Uric acid	Carbon nanofibers	0–5 mM	–	[41]
	Sweat	Cortisol	Carboxylate-rich pyrrole-derivative/ graphene	0–1 ng/mL	2.41 nA/mm^2	[42]
	Dopamine	Dopamine	Sn@GO/MnO_2	0–50 μM	92 μA/μM	[43]
	Biological fluids	Glycine	Quinoprotein	25–500 μM	0.881 nA/μM	[44]
	Sweat	Nicotine	CYP2B6	0–20 μM	4.3 nA/μM	[45]
DVP	Sweat	Uric acid	Graphene	0–100 μM	3.5 nA/μM	[9]
		Tyrosine		0–200 μM	0.61 nA/μM	
	Biological fluids	Uric acid	3D-printed graphene/ polylactic acid	0.5–250 μM	0.1723 μA/μM	[46]
		Nitrite			0.0031 μA/μM	
	Sweat	Lactate	AgNWs	1 μM–100 mM	–	[47]
	Blood serum	Uric acid	nanoflake-nanorod WS_2	5 μM–1 mM	312 nA/(nM^{-}·cm^2)	[48]
		Quercetin		10 nM–50 μM	258 nA/(nM·cm^2)	
	Serum	Glucose	Cu-xCu_2O NPs@3DG foam	0.8–10 mM	230.86 μA/(mM·cm^2)	[49]
	Sweat	Dipyridamole	Boron-doped diamond electrode	0.05–10 μM	–	[50]
		Acetaminophen		0.5–10 μM	–	
		Caffeine		0.5–10 μM	–	
	Staphyloco ccus aureus	*Staphyloco ccus aureus*	Bacterial cellulose/ carboxylated multiwalled carbon nanotubes	3–3 × 10^7 CFU/mL	–	[51]
	Epithelial-mesen chymal transition	Epithelial-mesen chymal transition	E-cadherin antibody-QD	1–900 ng/mL	0.01 μA/(ng·/mL^2)	[52]
Impedance	Tear	cortisol	Graphene field-effect transistor	0–40 ng/mL	1.84 ng/mL per 1% of the change in its resistance	[53]
	Aflatoxin B1 (AFB1)	AFB1	immunoassays with AFB1	1.56–31.2 ng/mL	8.74 kΩ/nM	[54]
Hybrid sensing	Perspiration	Na^+	Ionophore	10–160 mM	64.2 mV/decade	[6]
		K^+		1–32 mM	61.3 mV/decade	
		Glucose	GOx/PB	0–200 μM	2.35 nA/μM	
		Lactate	LOx/PB	0–30 mM	220 nA/mM	
	Sweat	Glucose	GOx/PB	25–300 μM	6.3 nA/μM	[55]
		Lactate	LOx/PB	5–35 mM	174 nA/mM	
		Ascorbic acid	Silk fabric–derived	20–300 μM	22.7 nA/μM	
		Uric acid	intrinsically nitrogen (N)– doped carbon textile	2.5–115 μM	196.6 nA/μM	
		Na^+	Ionophore	5–100 mM	51.8 mV/decade	
		K^+		1.25–40 mM	31.8 mV/decade	
	Sweat	Glucose	GOx/PB	0–200 μM	8 nA/μM	[56]
		Lactate	LOx/PB	0–25 mM	67 nA/mM	
		Na^+	Ionophore	5–160 mM	35 mV/decade	
		K^+		1–32 mM	45.5 mV/decade	
	Sweat	Glucose	GOx/SWCNTs/Chitosan	100–500 μM	0.714 nA/μM	[57]
		pH	PANI	3–8	60 mV/decade	
		Na^+	Ionophore	10–160 mM	60.1 mV/decade	
		K^+		2–32 mM	64.5 mV/decade	

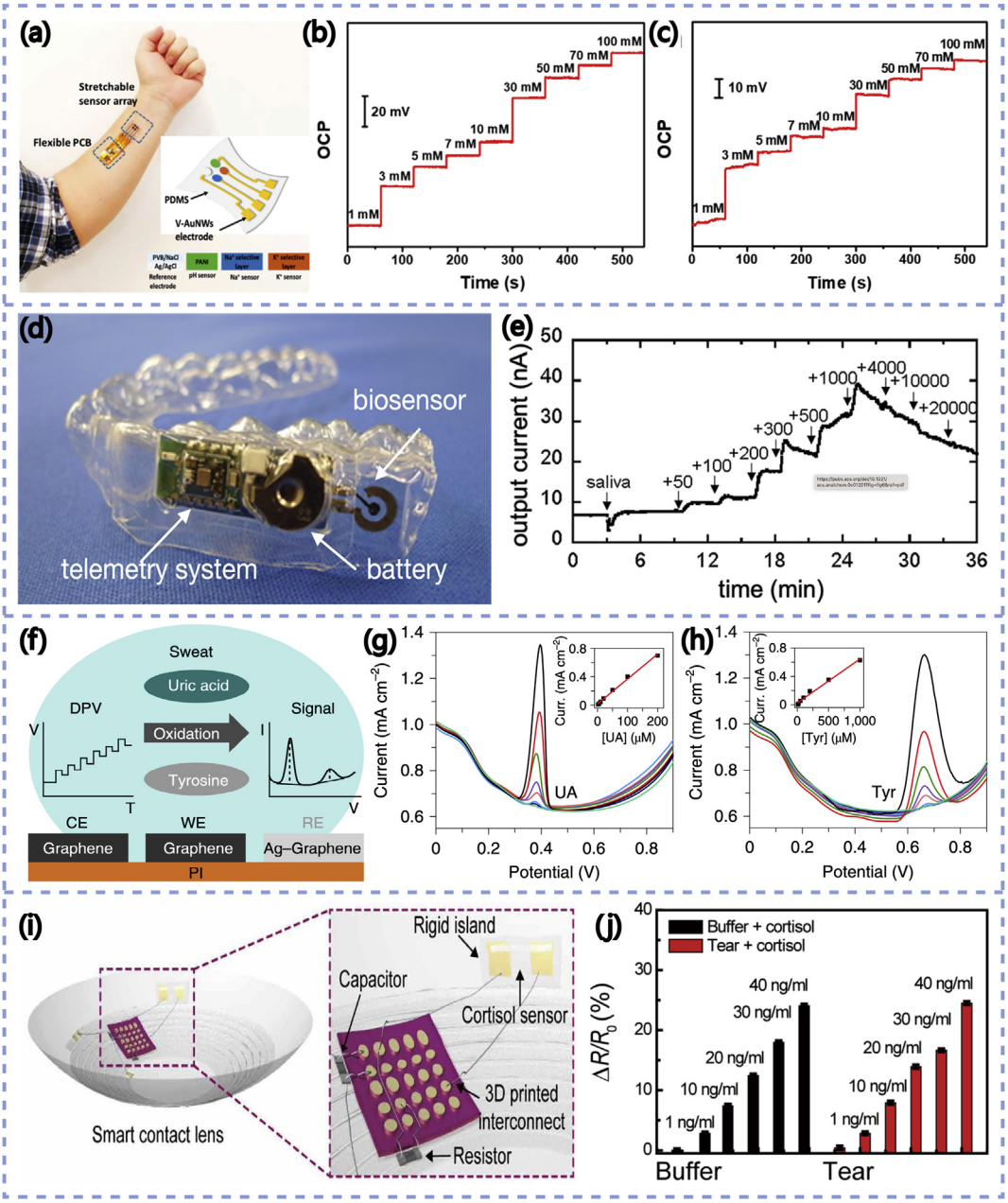

Fig. 2. Electrochemical biosensors based on different sensing modes. (**a**) A schematic of a stretchable sensor array. Open-circuit potential curves with different concentrations of Na^+ (**b**) and K^+ (**c**) [28]. (**d**) Photograph of the fabricated glucose sensor integrated with a wireless module and battery. (**e**) The performance of the glucose sensor [33]. (**f**) A three-electrode laser-engraved sweat sensor for simultaneous UA and Tyr detection. UA (**g**) and Tyr (**h**) detection with the laser-engraved sweat sensor [9]. (**i**) Schematic of the packaged smart contact lens integrated with the cortisol sensor. (**j**) Relative resistance changes as per the cortisol concentration in the buffer and the artificial tear solvent [53].

the electroactive substance is proportional to the concentration of electroactive products [59,60]. The current follows the Cottrell Eq. (2) as follows:

$$i(t) = \frac{nFAc_o{D_o}^{1/2}}{\pi^{1/2}t^{1/2}} \tag{2}$$

where I is the current at time t(s), n is the number of electrons, F is the Faraday constant, A is the geometric area of the electrode, c_o is the concentration of the oxidized species, and D_o is the diffusion coefficient of the oxidized species. In general, the amperometry-based biosensor is a three-electrode system including WE, RE, and counter electrode [27].

The amperometry method is often used for enzyme-based sensing, such as biosensors with glucose oxidase (GOx) and lactate oxidase (LOx) enzymes. Arakawa et al. [33] reported a saliva glucose sensor based on GOx (Fig. 2d). The sensor can quantify the glucose concentration in the range of 1.75–10,000 μmol/L, including the salivary sugar concentration of 20–200 μmol/L(Fig. 2e). In addition, the cellulose acetate film on the glucose sensor can inhibit the effects of ascorbic acid (AA) and UA in saliva. It can provide a useful method for unrestricted and non-invasive monitoring of saliva glucose for diabetic management.

Similar to the potentiometer test method, the amperometry provides straightforward strategy to convert the measurable current into the concentrations of the analytes. In addition, a

mediator layer can be adopted to lower down the potential required to trigger the oxidation/reduction reaction, thereby reducing power consumption. Although the enzymes provide excellent sensing selectivity, it could affect the sensor stability. Besides, the Faraday signal will decay over time, limiting the long-term monitoring reliability.

2.3. DPV mode

DPV uses amplitude pulses on a linear potential ramp, resulting in a staircase waveform, where the potential of each subsequent pulse is gradually higher than the previous pulse. The current is sampled again before the pulse is applied and after a predetermined time. Because the charging current is dissipated at a faster rate than the Faraday current generated by the redox reaction, DVP can minimize the capacitive current and perform better sensitivity [7,10]. DPV can also distinguish different analytes simultaneously by observing various redox processes. Cyclic voltammetry is usually used to initially explore the corresponding process reversibility and redox process types [11,61–63].

Because of its high detection accuracy, it has been reported for proteins and UA sensing. Yang et al. designed a completely laser-engraved sensor based on DVP testing to achieve continuous detection of low-concentration UA and tyrosine (Tyr) [9] (Fig. 2f). The detection sensitivity of UA and Tyr was 3.50 μA/(μM· cm^2) and 0.61 μA/(μM·cm^2), respectively (Fig. 2g and h). By using healthy volunteers and patients with gout to test the sensor, the test results can be correlated with the serum test results.

Although DVP can ensure sensing signal accuracy, low trace analytes detection and obtains information of multiple analytes at the same time by one scanning, it could trigger side reactions during the voltage scanning process and thus introduce signal interference. In addition, compared with the potentiometry and amperometry, this method requires relatively complex signal extraction and processing procedures.

2.4. Impedance sensing mode

Impedance sensing is to obtain the sensor resistance by applying a sinusoidal voltage to reflect the analyte concentration. As shown in Fig. 2i, Ku et al. [53] used graphene field-effect transistors to make a cortisol sensor with a detection limit of 10 pg/mL, which can detect the concentration of cortisol in human tears. The sensitivity of the sensors remains well after repeated testing in artificial tears or buffer (Fig. 2j). The *in vivo* test on live rabbits and human test proved that the sensor has good biocompatibility and reliability. However, this sensing mode requires relatively long detection time and complex data postprocessing process. Thus, it is not as widely adopted as the previous methods [11].

2.5. Hybrid sensing

To monitor the health of the human body more comprehensively, researchers have developed multianalyte sensing approaches. In 2016, Gao et al. [6] proposed a fully integrated sensor array for *in-situ* sweat analysis of multiple analytes, which can simultaneously selectively test glucose, lactic acid (amperometry), Na^+, and K^+ (potentiometry) in sweat (Fig. 3a). Later, He et al. [55] used nitrogen-doped graphite fabric as a WE to design a multiple sweat analysis patch that can simultaneously detect glucose, UA, lactic acid (amperometry), AA (DVP), Na^+, and K^+ (potentiometry) (Fig. 3b). Biosensors integrated with multiple sensing methods can better fulfill the practical personalized health monitoring, whereas it raises requirements for the sensing patch size miniaturization, stability of simultaneous operation of multiple sensors, and multiple signals processing.

3. Self-powered strategies for wearable biosensing applications

Self-powered and wearable biosensing devices harvest energy from the movement of the human body or the surrounding environment to support biosignal detection and transmission. The energy sources are currently used for self-powered and wearable biosensors mainly including mechanical, biofuel energy, and thermal energy collected on-body and solar energy harvested from the environment [10,16,64]. In this part, the research progress of wearable biosensors based on different energy harvesting methods is introduced (Table 2), together with the discussion on their advantages and challenges, respectively.

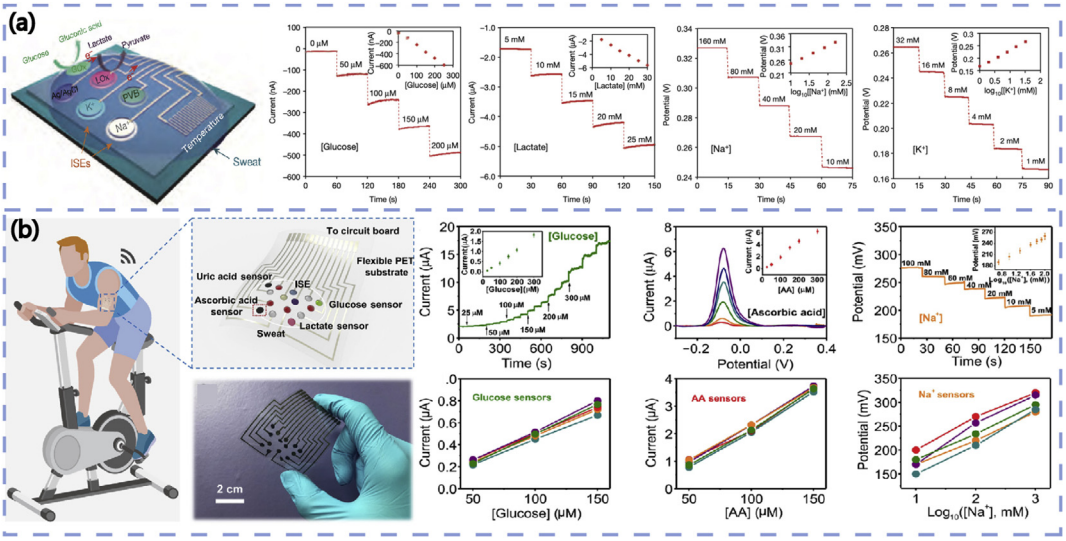

Fig. 3. Electrochemical biosensor array for hybrid sensing. (**a**) Fully integrated wearable sensor arrays for multiplexed *in situ* perspiration analysis [6]. (**b**) Integrated textile sensor patch for real-time and multiplex sweat analysis [55].

3.1. Triboelectric nanogenerators (TENGs)

The TENG is a mechanical energy-electrical conversion device based on frictional charging and electrostatic induction. Normally, it consists of two types of materials with different electron capture characteristics. The two counterparts will then carry different charges after contact and separation, thereby generating a potential difference on the surface [64,83]. When connected to an external circuit, it would generate a current.

TENGs have been widely reported for integration onto clothes for energy harvesting owing to friction between clothes when humans exercise [84,85]. Zhang et al. reported on the integration of TENGs between the inner shirt and the outer garment. The TENG was composed of copper film, polydimethylsiloxane (PDMS) film, and aluminum foil (Fig. 4a). Fig. 4b shows a uniform PDMS array on the copper film that improves triboelectric charging. When volunteers were exercising, the energy generated by the TENG could light up 30 light-emitting diodes (LEDs). At the same time, the TENG could harvest the energy generated by applause and store this energy with lithium-ion batteries. Clapping for 2 h at a frequency of 2 Hz could charge a lithium-ion battery from 440 to 880 mV (Fig. 4c). The battery was capable to power a glucose sensor [65]. This work demonstrates a strategy for integrating energy harvest devices, energy storage devices, and biosensors in the wearable platform. It also indicates that the energy of human motion can be used to support the biomarker detection.

With the popularity of mobile devices such as smartphones, the integration of wearable biosensors and wireless data transmission is a trend, whereas it poses higher requirements on the power supply. Gao and Zhang's groups proposed a free-standing triboelectric nanogenerator (FTENG) integrated with a microsweat sensor onto a flexible PCB (Fig. 4d and f). Polytetrafluoroethylene (PTFE) and copper were used for the friction pair of FTENGs. By chemically depositing Ni/Au in the electrode area and optimizing the interelectrode distance of the friction pair, a high-power output of 416 mW/m^2 was achieved. The energy harvested by the FTENG supports sweat sensing of pH and sodium ions (Fig. 4e) and drives the Bluetooth module to transmit human health-care information to smartphones. This work successfully demonstrated a wearable system that integrated energy harvesting, biosensors, and information transmission [19].

Table 2
Summary of self-powered wearable biosensors based on different energy harvesting strategies.

Powered supply unit	Sensors	Monitoring target	Position	Powered supply unit as a sensor	Output signal	References
TENGs	Glucose biosensor	Glucose	Inside clothes	No	Current generated by the biosensor	[65]
	Sweat biosensor	pH, Na^+	Waist	No	Voltage generated by the biosensor	[19]
	Sweat biosensor	Ca^{2+}	Arm, legs	Yes	Friction current	[66]
	Physical sensor	Motion state	Palm, foot, knee, elbow	Yes	Friction voltage	[67]
	Physical sensor	Pressure, temperature	Arm	Yes	Resistance, friction voltage	[68]
	Pressure sensor	Endocardial pressure	Endocardial	Yes	Friction voltage	[20]
PENGs	Pressure sensor	Motion state	Insole	Yes	Piezoelectric voltage	[69]
	Gesture sensor	Pressure, temperature	Finger	Yes	Piezoelectric voltage	[70]
	Physical sensor	Pressure, temperature, light	Hand	Yes	Piezoelectric current	[71]
	Perspiration sensor	Glucose, lactate, urea, uric acid	Wrist, forehead	Yes	Piezoelectric voltage	[18]
	Lactate sensor	Lactate	Joint	Yes	Piezoelectric voltage	[72]
	Urea/uric acid sensor	Urea, uric acid	Subcutaneous	Yes	Piezoelectric voltage	[17]
Biofuel cell	Sweat sensor	Lactate	Sock	Yes	Output voltage	[26]
	Urine sensors	Glucose	Diaper	Yes	Output voltage	[73]
	Glucose sensor	Glucose	–	Yes	–	[74]
	Sweat sensor	Glucose, lactate	Arm	Yes	Output voltage	[25]
	Sweat sensor	Glucose, urea, NH_4^+, pH	Arm, forehead	Yes	Output voltage	[75]
Solar cell	Sweat sensor	Glucose	Wrist	No	Current generated by the biosensor	[23]
	Heart rate sensor	Heart rate	Wrist	No	Current generated by the biosensor	[24]
	Glucose sensor	Glucose	Forehead	No	Current generated by the biosensor	[76]
	Physical sensor	Temperature, humidity, heart rate	Wrist	No	–	[77]
TEGs	ECG sensor	ECG	Arm	No	Voltage generated by the biosensor	[21]
	Physical sensor	Humidity, acceleration	Hand	No	–	[78]
		Identify materials, sense fluid flow		Yes	Output voltage	
PyEGs	Breath sensor	Temperature, breath statue	Mouth	Yes	Output voltage	[22]
	Breath sensor	Breath statue	Mouth	Yes	Output voltage	[79]
Sweat evaporation nanogenerator	Sweat sensor	Lactate	Forehead	Yes	Output voltage	[80]
Sweat flow nanogenerator	Sweat sensor	Lactate	Hand, chest	Yes	Output voltage	[81]
MEEG	Breath sensor	Motion state	Lips	Yes	Output voltage	[82]

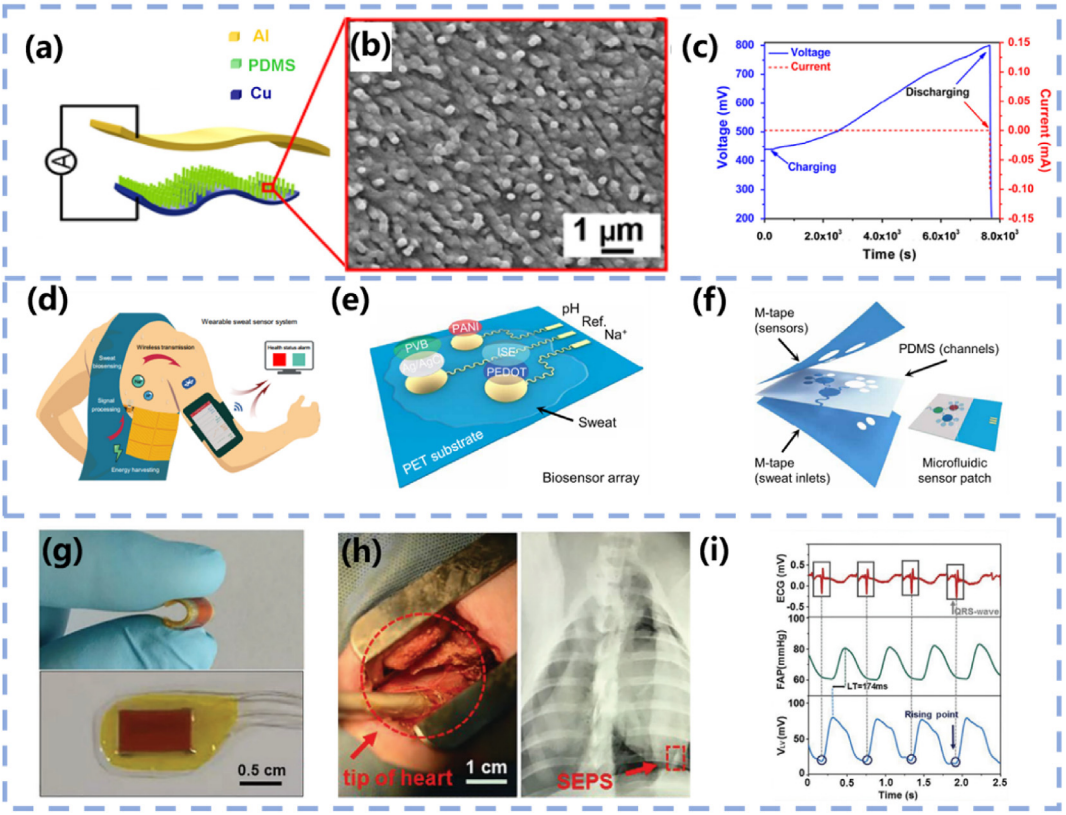

Fig. 4. TENGs for self-powered sensing systems. (**a**) Schematic illustration and (**b**) SEM image of the PDMS nanostructure array of a TENG built inside clothes for self-powered glucose biosensors. (**c**) The charging and the subsequent constant-current discharging curves of the integrated lithium-ion battery [65]. (**d**) Schematic diagram of a wearable sweat sensor-based FTENG system and (**e**) schematic illustration of the integrated sweat sensors on a flexible PET substrate with (**f**) microfluidic design for dynamic sweat sampling [19]. (**g**) Photograph of the self-powered endocardial pressure sensor and (**h and i**) its implantable applications for heart function monitoring [20].

In addition, TENGs can also be used for sensing. Zhao et al. proposed a self-powered biosensing electronic skin (e-skin) for real-time calcium ion (Ca^{2+}) detection in sweat. The e-skin is composed of polyaniline modified by nicotinamide adenine dinucleotide phosphate oxidase 5 (NOX5) and nicotinamide adenine dinucleotide phosphate (NADPH), PDMS and copper. Based on the frictional electrification/enzymatic reaction coupling effect, the sweat Ca^{2+} reacts with NOX5 and NADPH to generate additional current, and the current output could indicate the Ca^{2+} concentrations. At the same time, it can also be used as a power source to drive the entire system [66]. Kim et al. reported a polyimide/poly(vinylidene fluoride-trifluoroethylene) composite nanofiber-based TENG, which can collect energy from different parts of the human body (palm, foot, knee, and elbow). Meanwhile, the output voltage of each device can indicate the human body's movement state [67]. Rao et al. [68] prepared a TENG-based tactile sensor by introducing bismuth titanate (BaTiO) and reduced graphene oxide (rGO) in the microstructured PDMS, which can simultaneously monitor temperature and pressure while realizing energy conversion at the same time. The voltage output of the TENG varies when the contact area of the PDMS changes under different pressures. At the same time, the internal resistance of the BaTiO and rGO composites in the TENG changed with varying temperatures, thereby enabling temperature sensing. These works open up new possibilities for the development of e-skin that can realize multifunctional energy conversion and biosensing with a single device.

Apart from harvesting energy outside the body, TENGs can also be implanted inside the body. Liu et al. developed a miniaturized, flexible, and self-powered endocardial pressure sensor (SEPS) based on the TENG (Fig. 4g). The SEPS was composed of an encapsulation layer, electrode layer, triboelectric layer, and spacer layer. Three-dimensional ethylene-vinyl acetate copolymer film was used as a spacer layer, and Al foil layers were used to ensure effective contact and separation process. When the SEPS is compressed, the PTFE layer is in vertical contact with the Al layer. At the same time, owing to the difference in the triboelectric series, electrons flow into the nano-PTFE layer from the Al layer. With the release of the SEPS, the nano-PTFE film intends to return to its original position owing to its own elasticity. Once the two layers are separated, a potential difference is established between the two electrodes. Specifically, the fluctuation of endocardial pressure will cause the separation and contact process between the two triboelectric layers, which will cause the voltage on the external circuit to change periodically. The SEPS was integrated with a surgical catheter and was minimally invasively implanted into the left ventricle of the pig model (Fig. 4h). It can convert the energy of blood flow within the heart chambers into electricity. The sensor used the relationship between the endocardia pressure and the voltage output by the TENG to monitor the heart function for a long time (Fig. 4i). The linearity (R^2 = 0.99) with a sensitivity of 1.195 mV/mmHg was achieved [20]. This work provided new ideas for the application of TENGs in implantable biosensing.

In summary, TENGs are widely used in wearable self-powered sensors because of the relatively low manufacturing cost, light weight, high-output power density, and frequency independent. Whereas there also exist some critical issues: 1) the output current is low and might not be able to drive complex sensing systems; 2). the mechanical durability is also a challenge under friction. 3) the

energy collection based on TENGs relies largely on human movement, and thus the collected energy is very limited when people are at rest. It is necessary to develop reliable device packaging strategies to ensure the smooth functionality of TENGs in various scenarios. Meanwhile, it is possible to increase its output current with innovative materials or device structural design, so as to meet the needs of practical applications.

3.2. Piezoelectric nanogenerators (PENGs)

When an external force is applied to a piezoelectric material such as zinc oxide (ZnO), the mutual displacement of anions and cations occurs in the crystal to generate an electric dipole moment. It thereby generates a potential difference in the stretching direction of the material, which is known as the piezoelectric effect [86,87]. The PENG is a device that converts mechanical energy into electrical energy based on the piezoelectric effect of materials [88]. As human motion is one of the mechanical energy sources, PENGs have also attracted intensive research interest in fields of self-powered and wearable biosensing systems [89,90].

The PENGs can not only realize energy conversion but also serve as sensing components. For instance, it can be used to monitor pressure with its output voltage change. Yang et al. reported a flexible piezoelectric pressure sensor based on polydopamine (PDA)-modified $BaTiO_3$/polyvinylidene fluoride (PVDF) composite film (Fig. 5a) and applied for human motion monitoring. The device exhibited excellent piezoelectric properties owing to the excellent piezoelectric properties of PVDF and $BaTiO_3$ and the reduction of defects of the device by PDA modification. The device was integrated into the insole of a shoe. The varying pressure on the soles of the feet in different exercise states generated measurable output voltages, which enable action recognition such as jumping, walking, and running (Fig. 5b) [69].

Simultaneous monitoring of multiple physical signals is essential for future sensor systems, but a lot of work is only achieved by integrating multiple sensor types into a single device. However, single sensor multisignal monitoring can reduce the size of the sensor, which is essential for wearable sensors. Some researchers use materials that have both piezoelectric and pyroelectric properties to prepare wearable biosensors, which can sense pressure and temperature at the same time. For example, Yang et al. used graphene-doped PVDF fibers to make self-powered piezoelectric sensors (PESs). In addition to being sensitive to bending, owing to the pyroelectric properties of PVDF,

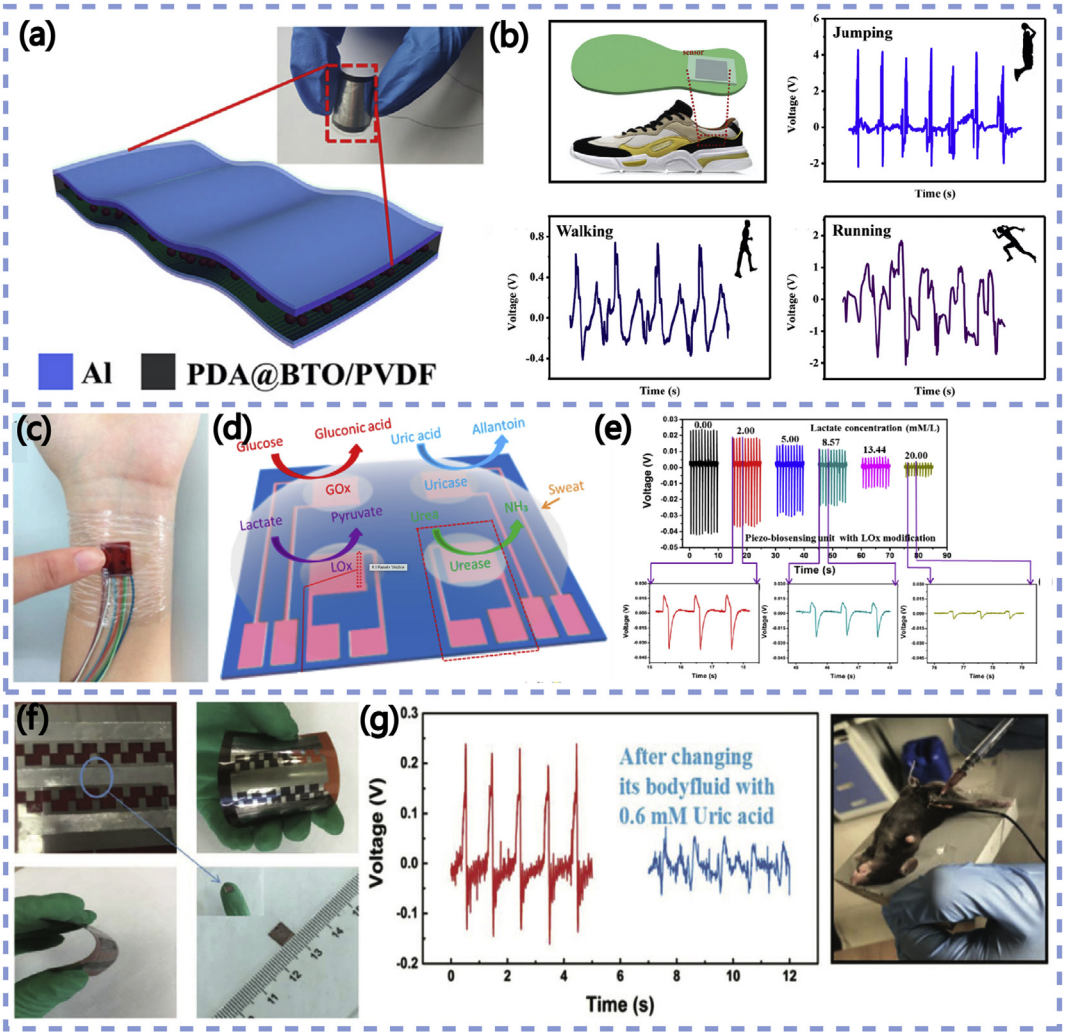

Fig. 5. PENGs for self-powered sensing systems. (**a**) The structure and (**b**) output of a flexible piezoelectric pressure sensor integrated into the insole of a shoe [69]. (**c**) Optical image and (**d**) schematic diagram of a self-powered wearable electronic skin for perspiration analysis based on piezo-biosensing. (**e**) The PENG generates a piezoelectric pulse after receiving external force with the change of lactate concentration [18]. Electronic skin for sweat analysis. (**f**) Optical picture and (**g**) the output piezoelectric voltage of a self-powered implantable electronic skin for *in situ* analysis of urea/uric acid in body fluids [17].

when it is close to a heat source, it can obtain a pyroelectric number to avoid burns. The integrated sensing system based on multiple PESs can accurately recognize the movement of each finger in real-time and can be effectively applied to sign language translation [70]. Zhao et al. used ferroelectric barium titanate film to prepare a self-powered multifunctional coupled sensor system. In addition to sensing temperature and pressure, the system can also accurately sense light. This is because under light conditions, the temperature of the device will rise, and the output current will always increase. When installed on a prosthetic hand, the flexible sensor system can detect the distribution of light, pressure, and temperature changes [71]. These strategies provide a new way for the development of e-skin.

Apart from monitoring the physical signal of the human body, the biosensing systems based on PENGs can be applied for chemical information detection. Han et al. developed a piezoelectric biosensor based on enzyme/ZnO nano-array and integrated it into a self-powered wearable e-skin (Fig. 5c). The e-skin-integrated biosensor array can simultaneously detect the content of lactate acid, glucose, UA, and urea in sweat (Fig. 5d). Based on the piezoelectric-enzyme-reaction coupling effect of enzyme/ZnO NWs, that is, the piezoelectric output depends on the enzymatic reaction between the enzyme and the corresponding perspiration component, the piezoelectric pulse indicates the physiological state of the human body when provided power supply at the same time (Fig. 5e) [18]. Similarly, Mao et al. [72] designed and prepared a PVDF/tetrapod-shaped ZnO/enzyme-modified nanocomposite film for human joint monitoring. It can detect changes in joint angles in human motion. The sensor modified by lactate oxidase (LOx) also had an obvious response to the change of lactate acid concentration. These sensors could realize real-time monitoring and analysis of athletes' training processes under non-invasive conditions.

On the other hand, the implantable application-based PENG can be realized by reasonable structural design. Yang et al. [17] reported an implantable e-skin for *in-situ* analysis of urea and UA in body fluids, which was made of ZnO NW modified enzyme (Fig. 5f). The output piezoelectric voltage served as both the signal of the biosensor and the power supply of the driving device (piezoelectric-enzyme-reaction coupling effect). The e-skin was implanted under the skin of the mouse's abdomen, and the urea and UA information of the mouse could be analyzed *in situ* (Fig. 5g).

PENGs are capable for high-output voltage supply. Similar to TENGs, they can serve as both energy units and sensors in self-powered sensing systems. Although they have been largely minimized in device volumes, their shortcomings of low output current and high output impedance need to be tackled.

3.3. Biofuel cells (BFCs)

BFCs are using enzymes as biocatalysts to convert biological energy into electrical energy [91]. The higher the analyte concentration, the greater the current generated by the reaction with the enzyme and the higher voltage output by the BFC. Biological fluids such as human sweat can be used as ideal and sustainable bioenergy for wearable devices.

Jeerapan et al. [26] designed a highly stretchable BFC with customized pressure ink by using screen printing (Fig. 6a). The BFC harvests energy from human sweat. Its output voltage signal is proportional to the concentration of the target analytes in the sweat. The BFC was integrated with socks to monitor the lactate concentration in volunteers' sweat (Fig. 6b). Fig. 6c shows that the sensor had a clear response to changes in the concentration of lactate with a maximum detection limit of 20 mM. In addition to the lactate acid-based BFC, other types of BFCs have also been studied. Zhang et al. reported a BFC-based self-powered biosensor system integrated with diapers to detect the composition of urine. The battery uses glucose in urine to react with GOx to generate electricity, and its output voltage is related to the concentration of glucose to monitor the level of glucose in human urine [73]. These studies demonstrated the potential application of the BFC for self-powered and wearable sensors, whereas the enzyme activity would limit the system's lifetime.

To tackle the limitation of system lifetime, Li et al. [74] developed an enzyme BFC based on metal-organic frame (MOF) to monitor the concentration of glucose in which the enzyme is immobilized in the MOF to achieve long-term stable monitoring (~15 h). Another novelty work offers another strategy. Bandodkar et al. [25] designed a BFC with replaceable enzyme-based sensors. The wearable biosensing patch powered by the BFC consists of a BFC sensor, colorimetric measurement, microfluidic channels, and low-power NFC (Fig. 6d). The sensor could transmit the detect information to the smart phone by the low-power NFC (Fig. 6e) within a maximum working distance of ~18 cm (Fig. 6f). The lactate-based BFC is illustrated in Fig. 6g. The microelectronic system and the microfluidic system were linked by a releasable magnetic coupling scheme, which facilitates the repeated use of the microelectronic system. This modular design could realize the reuse of expensive parts such as circuits.

In addition to the monitoring of a single target, the integration of multiple sensors is also concerned by more and more researchers. Yu et al. [75] reported a flexible and integrated e-skin driven by sweat based on a lactate fuel cell (Fig. 6h), which realizes multi-target monitoring by combining various sensor arrays including NH^{4+}, urea, glucose, and pH (Fig. 6i and j). In addition, the e-skin could monitor other physical parameters such as temperature, pressure, and muscle contractions. The e-skin has the potential to be applied in the wearable sensors owing to their test accuracy and wearing comfort.

BFCs can collect energy from human sweat compositions (e.g. lactate and glucose), which provide a convenient and sustainable method for on-body energy harvesting. However, biological fouling and inactivation of enzymes would affect its life span. In addition, the output voltage of BFCs is quite low, and the output power is unstable. Rational system design including device array construction would be one of the effective solutions. Besides, research efforts are expected to facilitate the charge transfer between the enzyme and the electrodes and optimize the catalyst performance. In addition, the biocompatibility of used materials and device durability should be taken into consideration, especially for wearable health-care applications.

3.4. Solar cells

Solar cells convert light energy into electricity [92]. It is usually connected to a battery [77] or supercapacitor [93,94] to compensate the interference of illuminance variation.

Solar cells are considered to be one of the ideal energy sources for self-powered wearable biosensors owing to their mature technology, clean energy sources, and small size. But light conditions will limit their work, so researchers often use rechargeable batteries to store the energy they collect to combat the impact of the environment. Zhao et al. [23] reported a photo-charging smartwatch that can continuously monitor the glucose content in sweat. The smartwatch was mainly composed of a glucose sensor, $Zn-MnO_2$ batteries, monocrystalline silicon solar cells, a printed circuit board (PCB), and a display screen (Fig. 7a). Among them, flexible solar cells were used for energy collection, and $Zn-MnO_2$ batteries store the energy collected by solar cells so that the device works normally in dark conditions. Fig. 7b shows that the sensor had a clear response to glucose concentration change. At the same

time, the display screen could also display the level of glucose concentration. This work innovatively integrated energy harvesting, storage, sensor system, and display system into a watch.

Apart from batteries, supercapacitors are also adopted in a self-powered system to store the energy collected by solar cells and fulfill the requirement of fast energy storage. Rajendran et al. prepared a flexible and stretchable supercapacitor by screen printing. The supercapacitor showed excellent mechanical properties under severe mechanical deformation conditions (Fig. 7c). It had an excellent power density (0.29 mW/cm^2) at a current density of 0.4 mA/cm^2. The solar cell was irradiated under a strong light to charge the supercapacitor for 5 min, which can light up the red LED light (Fig. 7e). Even in the case of weak sunlight (Fig. 7f), the supercapacitor could continuously drive the wearable pulse sensor through a customized low-power booster (Fig. 7d) [24]. The introduction of supercapacitors in the energy storage part of the system can meet the increasingly high energy demand of self-powered wearable biosensors in the future.

Enzyme-containing sensors have a limited use time, so Sun et al. [76] prepared a supercapacitor which was made of carbon fiber-based $NiCoO_2$ nanosheets with nitrogen-doped carbon (CF@$NiCoO_2$@N–C, Fig. 7g). It not only has an excellent performance (94% capacitance retention after 10,000 cycles) but also an outstanding flexibility (95% capacitance retention after 10,000 bending cycles). The supercapacitor stored energy collected from solar, and it could drive the portable workstation, Bluetooth module, and glucose sensor. The cathode (CF@$NiCoO_2$@N–C) of the supercapacitor could also be used as the enzyme-free WE in the glucose sensor owing to its electrocatalytic performance. The

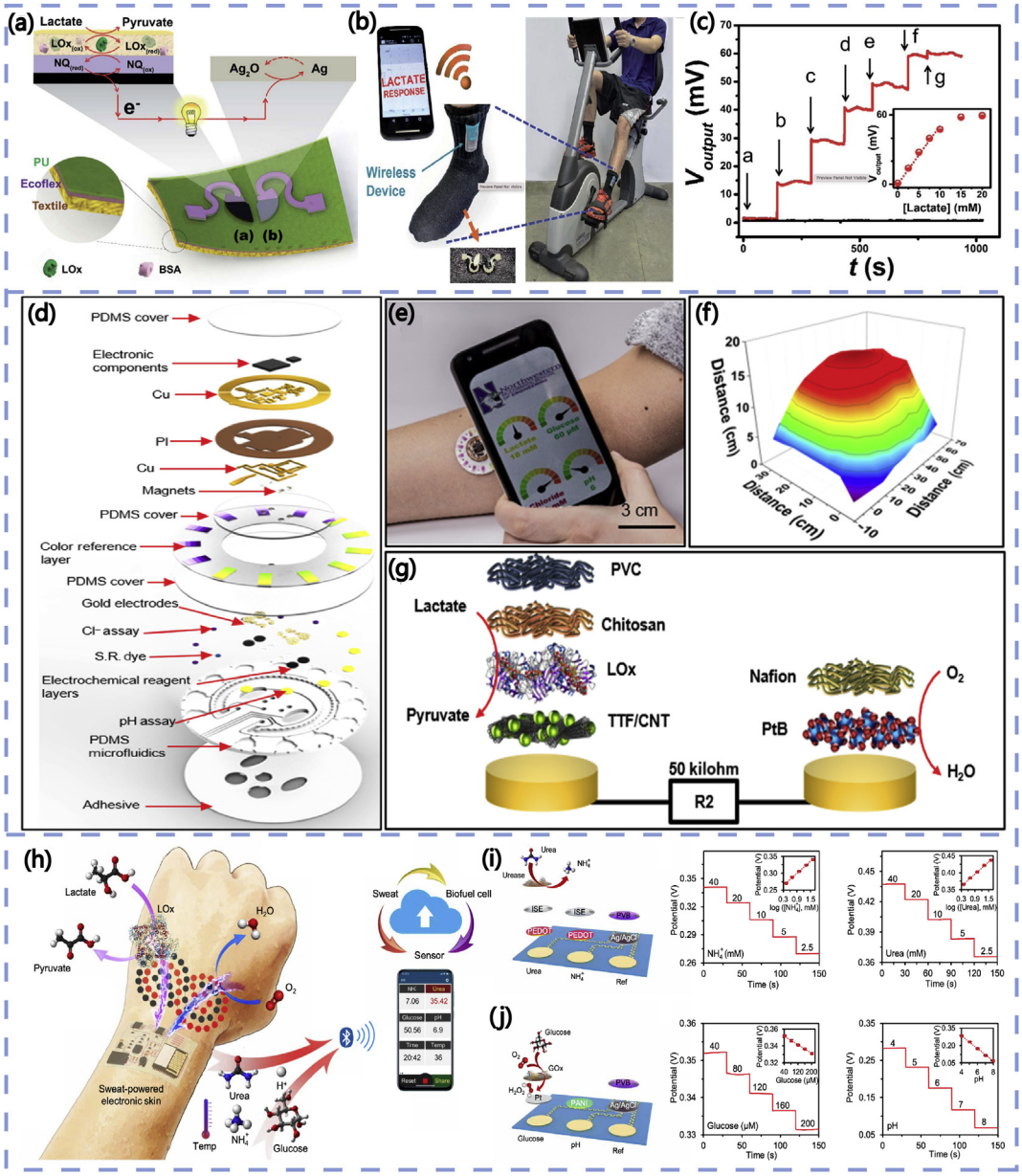

Fig. 6. BFCs for self-powered sensing systems. (**a**) The schematic illustration of a stretchable textile-based self-powered sensor with the BFC and (**b**) its integration on the socks for (**c**) lactate sensing [26]. (**d**) Schematic illustrating the exploded view of the complete hybrid battery-free system. (**e**) A phone interface that illustrates wireless communication and image acquisition. (**f**) Reading distance with a large NFC antenna. (**g**) Schematic illustration of the layered makeup of the biofuel cell-based lactate sensor [25]. (**h**) Working principal diagram of a biofuel-powered soft electronic skin. The integrated sensor array for simultaneous (**i**) urea and NH^{4+}, (**j**) glucose and pH monitoring and the performance [75].

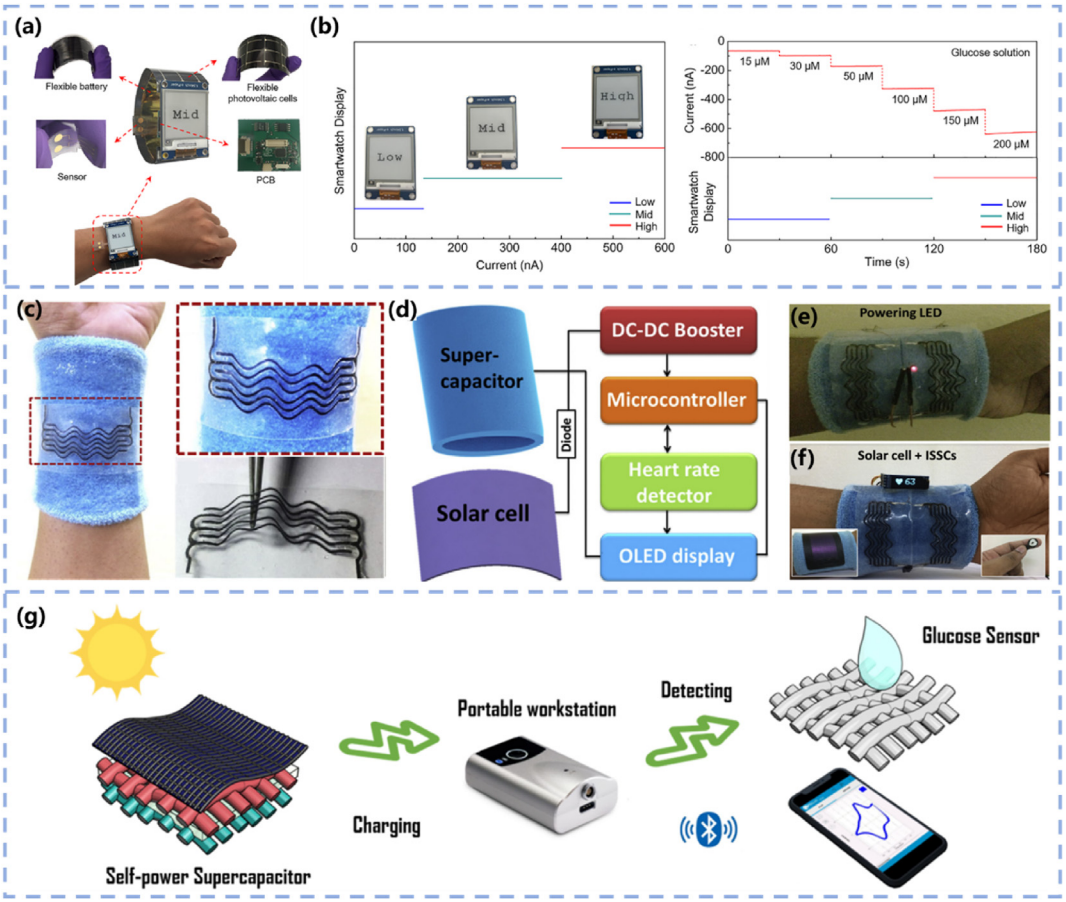

Fig. 7. Solar cells for self-powered sensing systems. (**a**) Images of self-powered glucose monitoring smartwatch and the components. (**b**) The glucose sensing response and the corresponding smartwatch display [23]. (**c**) Images of the self-powered wearable pulse rate sensor with wearable supercapacitor and the (**d**) systematic diagram. Photographs of the self-powered pulse rate sensor for real-time heart rate monitoring at (**e**) low intensity and (**f**) high intensity of illuminance [24]. (**g**) Schematic diagram of the self-powered wearable enzyme-free sensor [76].

strategy of enzyme-free biosensing would avoid the devices' lifetime limitation owing to enzyme activity loss.

For energy harvesting devices used in wearable devices, flexibility is one of its most important properties. However, many devices become unstable or even damaged under repeated bending conditions. Zhang et al. reported on a smart textile for generating electricity. The device integrates a solar cell and a rechargeable Zn−Mn battery. The battery is used to store excess energy to cope with non-light or low-light conditions. The use of fabric greatly improves the portability and comfort of the wearable device, and at the same time, it can work normally under twisted or humid conditions. The energy supply device can drive temperature sensors, humidity sensors, and heart rate sensors [77]. The combination of a energy harvesting device and fabric is an effective strategy to improve its flexibility and wearable comfort.

Solar energy harvesting and conversion technology are relatively mature, and their output power density is high. However, the solar energy input could be largely affected by time, weather, and surrounding environment. Thus, it is a commonly adopted strategy to combine solar cells with energy storage devices to ensure the continuous functionality of self-powered sensing devices. Further improvement on the conversion efficiency of flexible solar cells and the energy storage capability of the integrated batteries/supercapacitors are expected in the follow-up research.

3.5. Thermoelectric generators (TEGs)/pyroelectric generators (PyNGs)

Thermal energy is another ideal energy source for wearable devices [95–97]. It can convert heat generated by the human body into electricity to power wearable devices via Seebeck effect. Under heated conditions, when one of the materials is an n-type component and the other is a p-type component, the carriers of electrons and holes will move to the cold end and accumulate. If there is an external circuit connection, a current will be generated. The Seebeck effect causes an electric field proportional to the temperature gradient [98–100].

Kim et al. demonstrated a TEG-based wearable electrocardiogram system (Fig. 8a). To achieve high power generation and wearable comfortability, a polymer-based flexible heat sink composed of a super absorbent polymer and a fiber that promotes liquid evaporation were used. The power density of the TEG exceeded 38 μW/cm^2 in the first 10 min, and it exceeded 13 μW/cm^2 even after 22 h of continuous driving of the circuit, which is sufficient to continuously drive the entire sensor system [21]. Besides, the TEG itself can also serve as a sensor. A multifunctional e-skin was reported by Yuan et al. [78]. It is composed of p-type ($Bi_{0.5}Sb_{1.5}Te_3$) and n-type ($Bi_2Te_{2.8}Se_{0.2}$) thermoelectric crystal grains to enable high-thermoelectric conversion efficiency. To achieve desirable flexibility, the devices were assembled on a

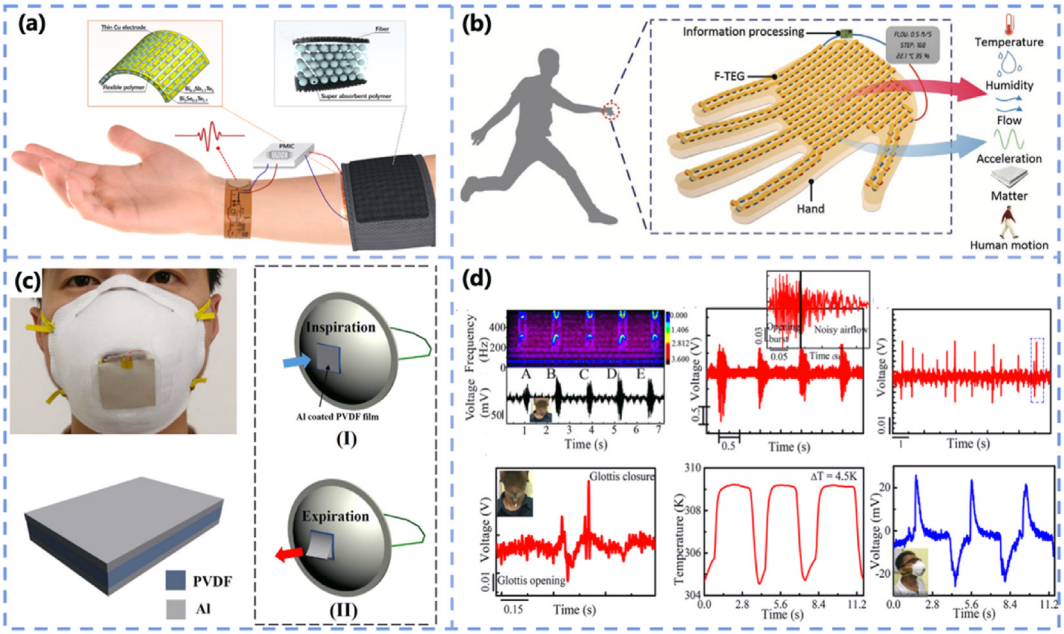

Fig. 8. TEGs/PyNGs for self-powered sensing systems. (**a**) Self-powered wearable electrocardiogram based on the TEG [21]. (**b**) A multifunctional self-powered electronic skin based on the TEG [78]. (**c**) The schematic of PyNG integrated on the mask [22]. (**d**) The performance of pyroelectric and piezoelectric hybrid nanogenerator for physiological signal monitoring [79].

flexible polyimide (PI) substrate (Fig. 8b). Except for human body heat collection to power the integrated hygrometer and accelerometer to monitor humidity and body movement acceleration, the e-skin can also detect the fluid flow because its output voltage changes with convective heat flux. This multifunctional self-powered e-skin provides an advantageous method for skin injury monitoring.

Body heat can also be collected with PyNGs, which are based on spontaneous polarization in anisotropic solids caused by temperature fluctuations to generate electric current. Traditional TEGs cannot work in a space with uniform temperature, whereas the PyNGs make up for this shortcoming [78,101,102]. Xue et al. integrated a PyNG composed of PVDF and aluminum into the N95 mask (Fig. 8c). A typical temperature fluctuation could be formed with the temperature difference between the human body and the surrounding environment, coupled with the phase change of the exhaled water vapor. This would then trigger the PyNG to generate voltage output that reflects the breathing state of the human body and the ambient temperature [22]. The PyNG can also be combined with other energy harvesting devices for wearable applications. Roy et al. designed a piezoelectric and thermoelectric hybrid nanogenerator. The hybrid nanogenerator is composed of PVDF and GO, so as to improve the pyroelectric energy collection and sensing performance of the device. The device can not only monitor the human body's coughing, swallowing, and joint movement but also monitor the breathing state through periodic temperature fluctuations during breathing (Fig. 8d) [79]. The facile fabrication process makes it promising for large-scale applications.

Because the human body generates heat all the time, thermal energy can be collected without interruption in theory. However, the temperature gradient between the human body and the surrounding environment might not be large enough for the TEGs/PyNGs to generate adequate power output density. Thus, research efforts on exploring novel functional materials to increase the energy conversion efficiency are desired. Besides, the combination with other energy harvesting methods could be another effective approach.

3.6. Other energy harvesting methods

In addition to the most commonly used energy harvesting methods described previously including TENGs, PENGs, solar cells, BFCs, and TEGs/PyNGs, there are also other energy harvesting methods, such as photoelectrochemistry devices [103], moisture generator [82], non-contact nanogenerator [105], and so on.

Guan et al. presented a self-powered wearable sweat-lactate sensor based on the coupling effect of sweat flow and lactate sensing (Fig. 9a). The biosensor was made of a porous carbon film modified by LOx. Fig. 9b shows that the carbon film was composed of interconnected carbon nanoparticles with nanoscale pores, which naturally absorb sweat from the skin. The natural evaporation of sweat could generate electricity and output voltage because the surface enzymatic reaction can change the zeta potential of carbon. The generated power can support wireless data transmission to external platforms (such as mobile phones, computers, and so on) [80]. Zhang et al. developed a wearable sweat sensor that does not require a battery or external power sources. It is mainly composed of a ZnO NW array modified by LOx and a flexible PDMS substrate. When it was attached to the skin, the sweat on the skin flows into the channel through capillary action. The continuous flow of droplets disrupts the balance of the electric double layer on the surface of ZnO NW and generates energy (hydraulic effect), which generates a potential difference between the upper and lower ends. At the same time, the reaction of LOx and lactate produces hydrogen peroxide, which affects the zeta potential of the ZnO NW surface (Fig. 9c). The output voltage showed a linear correlation with the sweat lactate acid concentration (Fig. 9d). The sensor can be used to monitor the physiological state of the human body during the exercise [81].

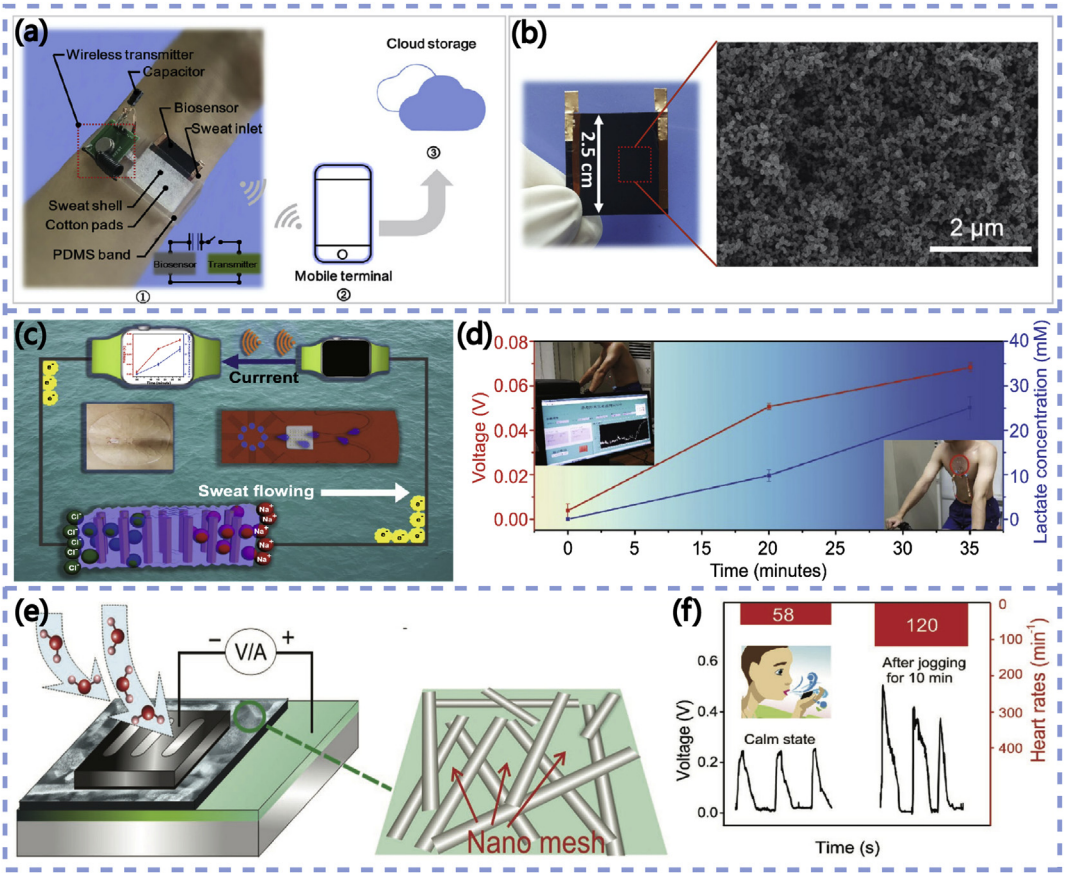

Fig. 9. Self-powered sensing systems based on hybrid energy harvesting. (**a**) The systematic diagram of a self-powered and wearable sweat lactate sensor. (**b**) Optical and SEM image of the porous carbon film modified by LOx for sweat absorption and lactate sensing [80]. (**c**) The working principal and (**d**) human subject sweat sensing results of a wearable and battery-free perspiration sensor powered by sweat flow and lactate sensing [81]. (**e**) The working principle and (**f**) the output voltage of a self-powered wearable breathing sensor based on the MEEG [82].

Another novel work was proposed by Guan et al. They developed a new type of generator, moisture-enabled electricity generator (MEEG) based on titanium dioxide (TiO_2) NW networks (TDNNs). The device collected energy from moisture (including moisture in human breath) to generate humidity-related voltage output. The power generation capacity of the TDNN MEEG was produced by the diffusion of water molecules along the many nanochannels existing in the NW network (Fig. 9e). When water molecules diffused into the narrowest channel, the diffusion of negative ions was hindered, and only positive ions with a smaller diameter continue to diffuse to generate voltage. Fig. 9f shows the change in the output voltage of the TDNN MEEG before and after running. Because the breathing speeded up after exercise, and the humidity in the exhalation was higher, the output voltage of the TDNN MEEG increased significantly. The device was successfully demonstrated for human respiratory monitoring, and it can also provide power for the commercial electronics, such as LEDs and high-power capacitors [82].

4. Power management strategy

Owing to various output power properties, including voltages and frequencies, rationally designed energy management strategies are required to ensure a stable power supply for wearable applications. In fact, most of the electronic devices and units used within the health-care sensing system are driven by the direct current (DC) power supply with the voltage of several volts. Therefore, the power conditioning and management modules normally include rectifiers, DC/DC converters, and capacitors/batteries, depending on the types of power source and power consumption requirement. Energy output from BFCs, TEGs, and solar cells is normally DC, which can directly charge the energy storage unit. On the other hand, rectification is needed for energy harvesters such as TENGs, PENGs, and PyNGs because of their alternating current (AC) behaviors. Some of the representative features of the widely used energy harvesting and conversion technologies for integration with wearable biosensing systems are summarized in Table 3.

Improvement on the energy utilization efficiency and rational power management strategies is applied in operation modes of the whole self-powered sensing systems, thus reducing the overall power consumption. Advanced sensing systems would adopt the microcontroller unit (MCU) to achieve control and coordination of different modules in the system including sensors, power supply, data processing, and communication. It also enables programmable controlling of the operation of the system, including the on/off setting and entering the sleep mode.

The following part of this chapter will focus on design and optimization from circuit to system architectural design of the self-powered sensing system. Details and classified discussion of power management for nanogenerators, BFCs, and solar cells are provided. Research progresses on system-level low-power consumption strategies is also presented.

Table 3
Features of the energy harvesting system.

Power supply unit	Sensors	Monitoring target	Size	Energy output	Position	Data readout	References
PENGs	Piezo-biosensor	Sweat (lactate, glucose, uric acid, urea)	1.4 × 1.5 cm^2	18.2 mV (@2 mM/L)	Wrist, forehead	–	[18]
	Piezo-biosensor	Urea/uric-acid	1 cm^2	0.41 V (@50 N, 0.1 mM)	Rat kidney	–	[17]
	Piezo-biosensor	Radial/carotid pulse	–	65 mV	Wrist, neck	Speakers	[106]
TENGs	Ion-selective electrodes	Sweat (pH, Na^+)	22.6 cm^2	~416 mW/cm^2	Arm	Bluetooth	[19]
	TENG-based sensor	Heart rate	1 × 1 cm^2 6.5 × 2 cm^2	2.28 mW	Arm (energy harvester) finger/wrist (sensor)	Bluetooth	[107]
	Triboelectric sensor	Motion; sweat (urea, uric acid, lactate, glucose, Na^+, K^+)	5 × 10 cm^2	~0.45 mA	Elbow	Green LEDs	[108]
	Triboelectric sensor	Endocardial pressure	1 × 1.5 cm^2	17.6–78.6 mV	Heart	–	[20]
	Electrochemical sensor	Glucose	2 × 7 cm^2 (energy harvester)	100 V	Clothes on the body (energy harvester)	–	[65]
Biofuel Cell	Electrochemical sensor; colorimetric assay	Sweat (pH, lactate, glucose, chloride)	32 mm diameter	–	Arm	NFC	[25]
	Ion-selective electrodes; strain sensors	Human motion; Sweat (urea, NH_4^+, glucose, pH)	–	~0.6 V (BFCs), ~3.3 V (DC/DC boost); ~ 3.5 mW/cm^2	Wrist, arm	Bluetooth	[75]
	Electrochemical sensor	Blood glucose	–	3.2 V; 0.225 mW/cm^2	–	–	[109]
	Electrochemical sensor	Sweat lactate	–	~1 mW/cm^2	Arm	Bluetooth/LED indicators	[110]
Solar Cell	SnO_2 Gas sensor	Ethanol/acetone	15 × 4 cm^2	2.8 V	Wrist	LED indicators	[94]
	Electrochemical sensor	Sweat glucose	28.44 cm^2	6.28 V	Wrist	E-ink display	[23]
PyNGs	Temperature sensor	Temperature	21 mm × 12 mm	0.215 mW/cm^2	–	LCD	[111]
TEGs	Temperature/humidity sensor, accelerometer	Temperature, humidity, acceleration	16 × 4 cm^2	3.1 μW/cm^2	Wrist	Smart watch (LCD)	[112]
	Electrocardiography	Electrocardiography	40 cm^2	38 μW/cm^2	Wrist/arm	Serial interface	[21]

4.1. Transformers for nanogenerators

Nanogenerators have proved their potential integration in energy harvesting in self-powered devices and systems. Nevertheless, owing to irregular and unstable electricity output, as well as low efficiency, nanogenerators are incapable of directly powering the traditional microelectronic device. Therefore, additional power conditioning units are needed. The following part of this section

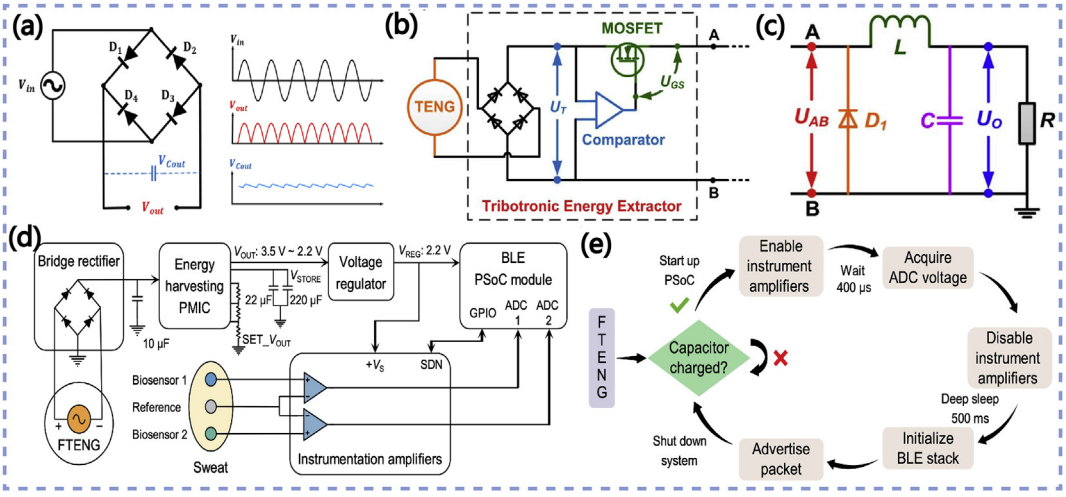

Fig. 10. Hardware design for nanogenerator-based energy supply systems. (**a**) Diode bridge rectifier and its electrical characteristics, (**b**) the energy extractor and (**c**) storage of a TENG power management system [126]. (**d**) Schematic diagram of a TENG powered sensor signal conditioning circuit and (**e**) power management strategies [19].

will mainly focus on research work on the power extraction, storage, and output reported in different nanogenerator-based energy supply systems.

Benefits from its large power density, high voltage output, good portability as well as simple structure [113], the TENG shows great application potential as an energy harvester and power supply in the area of wearable devices. Nevertheless, owing to irregular and unstable electricity output, the TENG is incapable of directly powering the traditional microelectronic device. During the past few years, tremendous efforts and trials have been made to improve the power conversion and storage performance of the TENG [114–120]. And based on these excellent power management strategies, the TENG-based energy supply systems and self-powered triboelectric biosensors become achievable.

As the simplest but effective conditioning circuit, the full-wave rectifier is commonly used to convert the bidirectional voltage input from the TENG into a direct, pulsating output voltage. Fig. 10a shows a simplified schematic diagram of the rectifier which consists of a four-diode bridge. For an AC voltage input, owing to the asymmetric conductance of the diode, the direction of current flowing through the output ends will keep the same, resulting in DC voltage output as shown in the right part of Fig. 10a. Furthermore, the connection of a capacitor in parallel at the output terminal achieves storage of energy output from the TENG, which will not only smoothen the voltage output V_{Cout} but also enable continuous and regular power supply. Taking advantage of its simple architecture and stable energy output, such a system is widely used in many self-powered biosensing and wearable electronics designs. A TENG cloth with a lithium-ion battery is reported to be able to power a Bluetooth-enabled heartbeat meter [121]. The battery is charged by the rectified energy output from the TENG with a voltage of 1.9 V and then galvanostatically discharged to power peripheral electronics. Other electronic devices such as LEDs [122] and electronic calculators [123] are also demonstrated using the rectifier and capacitor to achieve TENG power conversion, storage, and output.

On the other hand, huge output impedance and low output current of the TENG still restrict its usage for powering devices with low impedance [124]. As reported by Zhu et al. [125], a 40:1 transformer was introduced between the TENG and rectifier to achieve a higher current. Advanced power management strategies are further proposed, among which the switch plays a vital role in promoting the power extraction and conversion efficiency of TENG systems. Niu et al. [120] proposed a power management circuit to achieve 60% efficiency, which uses electronic switches, inductors, and a temporary capacitor to avoid impedance mismatching between the TENG and energy storage unit. Xi et al. [126] further proposed a universal power management strategy with 80% efficiency and 1 MΩ impedance. As shown in Fig. 10b, the comparator compares the rectified voltage with the reference voltage which is presented as per the peak voltage of peak open-circuit voltage of the TENG and controls the on- and off-state of the metal-oxide-semiconductor field-effect transistor. This achieves maximized power transfer from the TENG to back-end circuit. Further in Fig. 10c, a logic circuit is designed to store the energy. And powering devices such as a calculator and watch are achieved. Beyond this, William Harmon et al. [127] further proposed a buck converter in which the silicon-controlled rectifier and Zener diode are used to control the energy flow between the TENG and the energy storage unit.

Moreover, system-level integration of self-powered sensor systems is reported which consist of an energy harvester, power management unit, signal processing unit, and data communication module. A self-powered biosensing is achieved by combining the triboelectric energy harvester with the ion-selective electrode-based sweat biosensor [19]. A power management module (S6AE101A, Cypress Semiconductor) is used, followed by a voltage regulator (TPS7A05, Texas Instruments) to realize a 2.2 V output. Energy from the TENG further powers the Bluetooth module and amplifiers to enable amplifying, processing, and readout of sensing signals. Besides, low power consumption devices, and efficient power management strategies are adopted. As shown in Fig. 10e, each module can be waked up or shut down at different stages of the operation cycle of biosensing, controlled by a programmed system on chip to avoid energy waste. And harvested energy powers 18 such working cycles after 60-min running with constant speed. In this full integration system, a wearable triboelectric energy harvester with a conditioning circuit enables stable power supply to both the sensors and peripheral electronic devices; low power circuit design combined with optimal power management strategies further improves the efficiency and lifetime of such a self-powered sensor system. Other several works [107,121,128] are also reported with the TENG-powered integration sensing system.

Similarly, extracting energy from motion sources, PENGs and self-powered sensors transform Kinect energy into electric energy and output in the form of alternating voltage [129,130]. Therefore, the simplest bridge rectifier enables AC/DC converting, combining with optimized energy extractor to overcome the impact of large output impedance and further enhance the energy transfer efficiency, a power conditioning unit for the PENG can be realized then. Moreover, hybrid designs are further reported to integrate different nanogenerators into one system to achieve more effective energy harvesting [131–133]. Cooperation of PENG and TENG harvests more energy during single motion and thus enables high power output [134].

4.2. Increasing power density of BFCs output

Human body fluids serve as a good bioenergy source, enabling energy harvesting and power supply during body fluid-based electrochemical sensing [25,110,135–138]. Although direct current output can be obtained from the BFC, its relatively low voltage output fails to directly drive electronic devices like LED displays [136]. Therefore, extra energy management modules, such as the charge pump of the DC boost converter, are needed.

Slaughter et al. [109] apply the charge pump circuit to a self-powered glucose sensing system, which not only boosts the output voltage but also converts the glucose concentration information into an electric signal. As shown in Fig. 11a, the charge pump is a kind of DC/DC converter, of which the energy is stored first and then released in a controlled manner to obtain the required output voltage. From the charge pump circuit, a 0.25 V input voltage signal is converted into 1.2–1.8 V pulse wave voltage output. Further boosted by a DC boost converter, a 3.3 V steady DC output can be obtained, which can be used to drive a commercial glucometer. Yu et al. [75] further proposed an energy control flow to enable low power consumption. An operation circle is shown in Fig. 11b, during which the bluetooth low energy (BLE) and (analog-to-digital converter) ADC modules alternate between waking-up and deep sleep modes. Other power management methods are also reported in an on-chip integration of self-powered biosensors [139,140]. To enable longevity of the BFC, the energy circuit only operated at the maximum power point at a very narrow duty cycle to extract enough energy, while working at a low-power mode most of the time. Benefiting from these power conversion and management designs, the bio-fuel cell-based self-powered sensing system is expected to have wide applications in the wearable health monitoring industry.

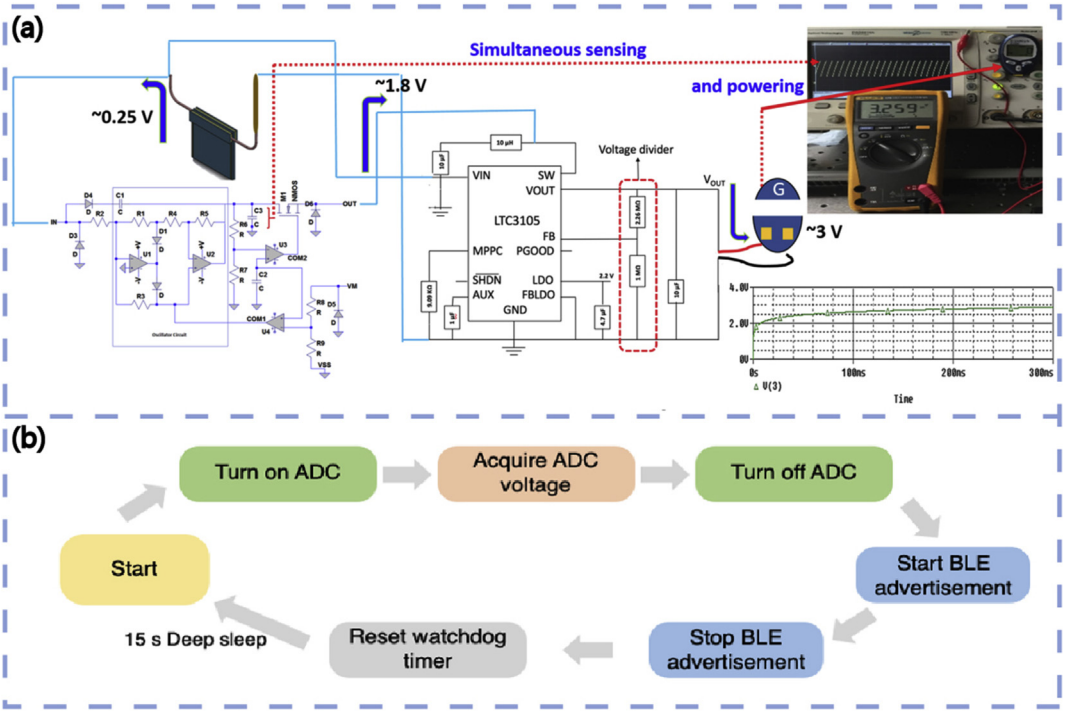

Fig. 11. Energy management strategies for BFC-based sensing systems. (**a**) Bio-fuel cell enabled self-powered sensor system with charge pump and DC boots converter [109]. (**b**) Optimized power management for the biofuel cell-powered sensor system.

4.3. Elimination of environmental disruption for solar energy

Generally, the solar cell converts the energy of light into a DC voltage output and subsequently charges the supercapacitor or battery, so as to provide continuous and stable power supply with eliminated interference by environmental illuminance. The ADC boost converter can be used to improve the driving capability of a solar cell power system.

Proposed by Zhao et al. [29], flexible photovoltaic cells and batteries are used to fully power a smartwatch for sweat glucose sensing. The solar cell can generate an open circuit voltage of 6.28 V under air mass 1.5 (AM1.5) while 5.12 V under the low intensity of light. And the battery is charged up to 6 V to drive the E-ink display and signal processing circuit for sensors. Rajendran et al. [24] demonstrate a self-powered system in which a supercapacitor can be charged to 1.7 V within several hundred seconds by the solar cell, with a low-power DC-DC converter (BQ25504, Texas Instruments) further boosts the output voltage to about 5.2 V (Fig. 12a–b). Noted that because of the dependence of light of the solar cell, larger energy storage capability, and rational power management strategy for the self-powered system will be crucial in continuous healthcare monitoring.

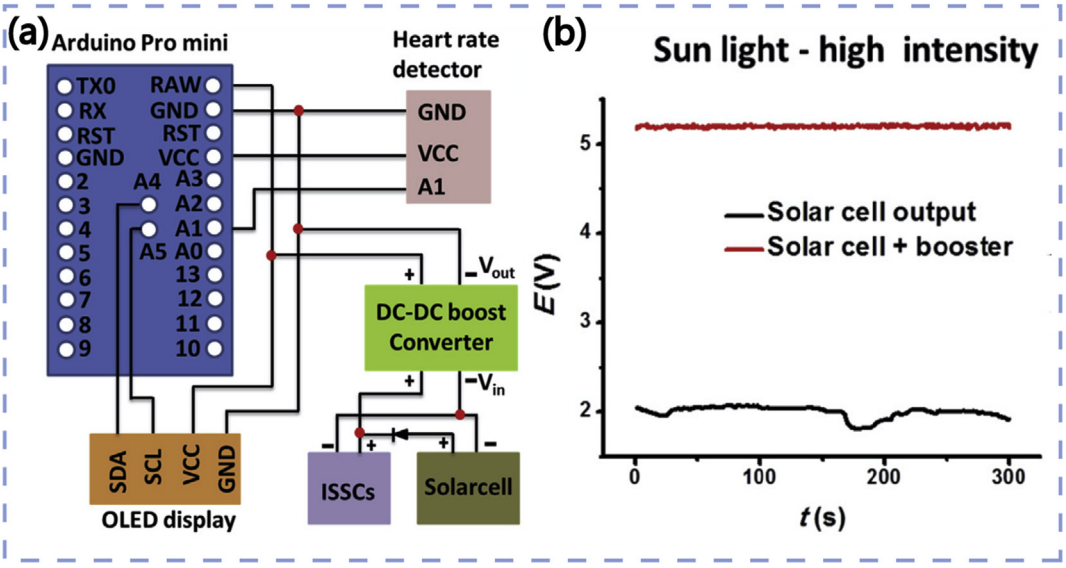

Fig. 12. (**a**) Circuit design for the solar cell-based self-powered sensors and (**b**) the voltage output of it [24].

4.4. System-level strategies toward low-power consumption design

With increasing needs of the intelligence biosensing system in healthcare, more complex electrocircuit and devices are used to enable better man-machine interface, which on the other hand increase the power consumption of the whole self-powered health monitoring system. Therefore, system-level low power consumption optimization becomes the key to extend the battery life. Following of this part will mainly focus on power managements in the operation of the system.

The power consumption largely depends on the biosensing scenarios. For continuous monitoring, data need to be measured and extracted in real-time. Nevertheless, units such as memory, MCU, data-processing circuit, readout module, and power supply module do not have to turning on all the time. In each measuring cycle, the on/off states of each module can be fine programmed to lower down the power consumption, especially in the on-chip integrated sensing system with the application-specific integrated circuit [141–143]. For sensing systems without real-time or continuous monitoring, the whole system can be turned off or switched to deep sleep mode when measurement is not required. When the system goes into deep sleep mode, most of the peripheral devices will be powered off to reduce the power consumption. Circuit current during deep sleep mode can be as low as ~2 μA [19]. The system in sleep mode can be waked up both by internal timer or external signal. Therefore, the operation of a healthcare sensing system can be not only fine programmed to fulfill the application requirements but also ensure a long battery life. Moreover, for the wireless communication module used in some wireless health monitoring systems, power consumption can be further decreased by adopting NFC which enables energy harvesting from the RF filed [144,145].

5. Challenge and outlook

Wearable biosensors can detect physical and physiological biosignals in a minimal/non-invasive manner. To achieve continuous and real-time monitoring of body status, wearable biosensing systems with self-powered capability are highly desired. The rapid research advance in flexible and miniaturized energy devices has greatly push forward the integration of self-powered technologies into wearable electronics. Although most of the biosensors for health-care applications have low power consumptions, the entire biosensing systems that realize data extraction, analysis, transmission, and display pose relatively high requirements for power supply.

So far research advances in material engineering and device fabrication technologies greatly contribute to the development of energy devices with attractive form factors, including miniaturized device sizes, high-power conversion efficiency, and energy storage capacity. Energy harvesting and storage devices have also been fabricated into a variety of flexible platforms, including fibers and textiles, with largely enhanced performances that are competitive with rigid devices. However, it is still challenging to ensure a stable and high-efficient power output, mainly owing to the unavoidable interference from body movements, mechanical frictions, and environmental factors.

On the one hand, rational packaging strategies of each individual device and the entire wearable biosensing systems should be adopted. For instance, electrolyte leakage or solvent evaporation in batteries or supercapacitors can be eliminated with proper package, so as to remain their energy storage capacity and device lifetime. On the other hand, integration of individual biosensor, energy device, and component (such as sensing signal conditioning and readout modules) via external connections could introduce impedance, which could result in extra power consumption and lower down power efficiency. Besides, undesirable noise could be generated, which would largely interfere with the biosensing signals. To tackle this challenge, innovation on system configuration and high-thoughtput fabrication methods are required to achieve monolithic fabrication and integration of power management circuits and supporting components into the wearable platforms.

Overall, research efforts in self-powered and wearable biosensors aim at the destination of monitoring human health status in real-time, wireless signal transmission, and convenient data visualization on mobile devices. Meanwhile, it is expected to provide accurate and reliable information to build personalized health profiles and support remote clinical diagnosis. With the rise of on-chip integrated systems, battery-free devices, and advanced power management approaches, the entire wearable systems will not doubt become smaller in size with enhanced biosensing stability and operation duration. Moreover, the innovation on new materials with attractive factors like breathable and washable properties would improve the wearing comfort properties of such devices and promote their practical applications in personalized healthcare.

Declaration of competing interest

The authors declare that they have no known competing financial interests or personal relationships that could have appeared to influence the work reported in this paper.

Acknowledgments

This work was supported by the Engineering Research Center of Integrated Circuits for Next-Generation Communications Grant (Y01796303), Southern University of Science and Technology Grant (Y01796108, Y01796208), and NSQKJJ (K21799122, K21799109).

References

[1] Y. Zhao, B. Wang, H. Hojaiji, Z. Wang, S. Lin, C. Yeung, H. Lin, P. Nguyen, K. Chiu, K. Salahi, X. Cheng, J. Tan, B.A. Cerrillos, S. Emaminejad, A wearable freestanding electrochemical sensing system, Sci. Adv. 6 (12) (2020), eaaz0007, https://doi.org/10.1126/sciadv.aaz0007.

[2] J.R. Sempionatto, T. Nakagawa, A. Pavinatto, S.T. Mensah, S. Imani, P. Mercier, J. Wang, Eyeglasses based wireless electrolyte and metabolite sensor platform, Lab Chip 17 (10) (2017) 1834–1842, https://doi.org/10.1039/c7lc00192d.

[3] T. Arakawa, Y. Kuroki, H. Nitta, P. Chouhan, K. Toma, S. Sawada, S. Takeuchi, T. Sekita, K. Akiyoshi, S. Minakuchi, K. Mitsubayashi, Mouthguard biosensor with telemetry system for monitoring of saliva glucose: a novel cavitas sensor, Biosens. Bioelectron. 84 (2016) 106–111, https://doi.org/10.1016/j.bios.2015.12.014.

[4] J. Kim, S. Imani, W.R. de Araujo, J. Warchall, G. Valdes-Ramirez, T.R. Paixao, P.P. Mercier, J. Wang, Wearable salivary uric acid mouthguard biosensor with integrated wireless electronics, Biosens. Bioelectron. 74 (2015) 1061–1068, https://doi.org/10.1016/j.bios.2015.07.039.

[5] H.Y. Nyein, W. Gao, Z. Shahpar, S. Emaminejad, S. Challa, K. Chen, H.M. Fahad, L.C. Tai, H. Ota, R.W. Davis, A. Javey, A wearable electrochemical platform for noninvasive simultaneous monitoring of Ca^{2+} and pH, ACS Nano 10 (7) (2016) 7216–7224, https://doi.org/10.1021/acsnano.6b04005.

[6] W. Gao, S. Emaminejad, H.Y.Y. Nyein, S. Challa, K. Chen, A. Peck, H.M. Fahad, H. Ota, H. Shiraki, D. Kiriya, D.H. Lien, G.A. Brooks, R.W. Davis, A. Javey, Fully integrated wearable sensor arrays for multiplexed in situ perspiration analysis, Nature 529 (7587) (2016) 509–514, https://doi.org/10.1038/nature16521.

[7] J. Kim, A.S. Campbell, B.E. de Avila, J. Wang, Wearable biosensors for healthcare monitoring, Nat. Biotechnol. 37 (4) (2019) 389–406, https://doi.org/10.1038/s41587-019-0045-y.

[8] Y. Yang, W. Gao, Wearable and flexible electronics for continuous molecular monitoring, Chem. Soc. Rev. 48 (6) (2019) 1465–1491, https://doi.org/10.1039/c7cs00730b.

[9] Y. Yang, Y. Song, X. Bo, J. Min, O.S. Pak, L. Zhu, M. Wang, J. Tu, A. Kogan, H. Zhang, T.K. Hsiai, Z. Li, W. Gao, A laser-engraved wearable sensor for

sensitive detection of uric acid and tyrosine in sweat, Nat. Biotechnol. 38 (2) (2020) 217–224, https://doi.org/10.1038/s41587-019-0321-x.
[10] R.C. Reid, I. Mahbub, Wearable self-powered biosensors, Curr. Opin. Electrochem. 19 (2020) 55–62, https://doi.org/10.1016/j.coelec.2019.10.002.
[11] M. Bariya, H.Y.Y. Nyein, A. Javey, Wearable sweat sensors, Nat. Electron. 1 (3) (2018) 160–171, https://doi.org/10.1038/s41928-018-0043-y.
[12] J. Liu, Z. Geng, Z. Fan, J. Liu, H. Chen, Point-of-care testing based on smartphone: the current state-of-the-art (2017-2018), Biosens. Bioelectron. 132 (2019) 17–37, https://doi.org/10.1016/j.bios.2019.01.068.
[13] S. Patel, H. Park, P. Bonato, L. Chan, M. Rodgers, A review of wearable sensors and systems with application in rehabilitation, J. NeuroEng. Rehabil. 9 (2012) 21, https://doi.org/10.1186/1743-0003-9-21.
[14] L.-C. Tai, T.S. Liaw, Y. Lin, H.Y.Y. Nyein, M. Bariya, W. Ji, M. Hettick, C. Zhao, J. Zhao, L. Hou, Z. Yuan, Z. Fan, A. Javey, Wearable sweat band for noninvasive levodopa monitoring, Nano Lett. 19 (9) (2019) 6346–6351, https://doi.org/10.1021/acs.nanolett.9b02478.
[15] Y. Lin, M. Bariya, H.Y.Y. Nyein, L. Kivimäki, S. Uusitalo, E. Jansson, W. Ji, Z. Yuan, T. Happonen, C. Liedert, J. Hiltunen, Z. Fan, A. Javey, Porous enzymatic membrane for nanotextured glucose sweat sensors with high stability toward reliable noninvasive health monitoring, Adv. Funct. Mater. 29 (33) (2019) 1902521, https://doi.org/10.1002/adfm.201902521.
[16] Y. Tang, X. Li, H. Lv, W. Wang, C. Zhi, H. Li, Integration designs toward new-generation wearable energy supply-sensor systems for real-time health monitoring: a minireview, Infomat 2 (6) (2020) 1109–1130, https://doi.org/10.1002/inf2.12102.
[17] W. Yang, W. Han, H. Gao, L. Zhang, S. Wang, L. Xing, Y. Zhang, X. Xue, Self-powered implantable electronic-skin for in situ analysis of urea/uric-acid in body fluids and the potential applications in real-time kidney-disease diagnosis, Nanoscale 10 (4) (2018) 2099–2107, https://doi.org/10.1039/c7nr08516h.
[18] W. Han, H. He, L. Zhang, C. Dong, H. Zeng, Y. Dai, L. Xing, Y. Zhang, X. Xue, A self-powered wearable noninvasive electronic-skin for perspiration analysis based on piezo-biosensing unit matrix of enzyme/ZnO nanoarrays, ACS Appl. Mater. Interfaces 9 (35) (2017) 29526–29537, https://doi.org/10.1021/acsami.7b07990.
[19] Y. Song, J. Min, Y. Yu, H. Wang, Y. Yang, H. Zhang, W. Gao, Wireless battery-free wearable sweat sensor powered by human motion, Sci. Adv. 6 (40) (2020), eaay9842, https://doi.org/10.1126/sciadv.aay9842.
[20] Z. Liu, Y. Ma, H. Ouyang, B. Shi, N. Li, D. Jiang, F. Xie, D. Qu, Y. Zou, Y. Huang, H. Li, C. Zhao, P. Tan, M. Yu, Y. Fan, H. Zhang, Z.L. Wang, Z. Li, Transcatheter self-powered ultrasensitive endocardial pressure sensor, Adv. Funct. Mater. 29 (3) (2019) 1807560, https://doi.org/10.1002/adfm.201807560.
[21] C.S. Kim, H.M. Yang, J. Lee, G.S. Lee, H. Choi, Y.J. Kim, S.H. Lim, S.H. Cho, B.J. Cho, Self-powered wearable electrocardiography using a wearable thermoelectric power generator, ACS Energy Lett. 3 (3) (2018) 501–507, https://doi.org/10.1021/acsenergylett.7b01237.
[22] H. Xue, Q. Yang, D. Wang, W. Luo, W. Wang, M. Lin, D. Liang, Q. Luo, A wearable pyroelectric nanogenerator and self-powered breathing sensor, Nano Energy 38 (2017) 147–154, https://doi.org/10.1016/j.nanoen.2017.05.056.
[23] J. Zhao, Y. Lin, J. Wu, H.Y.Y. Nyein, M. Bariya, L.C. Tai, M. Chao, W. Ji, G. Zhang, Z. Fan, A. Javey, A fully integrated and self-powered smartwatch for continuous sweat glucose monitoring, ACS Sens. 4 (7) (2019) 1925–1933, https://doi.org/10.1021/acssensors.9b00891.
[24] V. Rajendran, A.M.V. Mohan, M. Jayaraman, T. Nakagawa, All-printed, interdigitated, freestanding serpentine interconnects based flexible solid state supercapacitor for self powered wearable electronics, Nano Energy 65 (2019) 104055, https://doi.org/10.1016/j.nanoen.2019.104055.
[25] A.J. Bandodkar, P. Gutruf, J. Choi, K. Lee, Y. Sekine, J.T. Reeder, W.J. Jeang, A.J. Aranyosi, S.P. Lee, J.B. Model, R. Ghaffari, C.-J. Su, J.P. Leshock, T. Ray, A. Verrillo, K. Thomas, V. Krishnamurthi, S. Han, J. Kim, S. Krishnan, T. Hang, J.A. Rogers, Battery-free, skin-interfaced microfluidic/electronic systems for simultaneous electrochemical, colorimetric, and volumetric analysis of sweat, Sci. Adv. 5 (1) (2019), eaav3294, https://doi.org/10.1126/sciadv.aav3294.
[26] I. Jeerapan, J.R. Sempionatto, A. Pavinatto, J.-M. You, J. Wang, Stretchable biofuel cells as wearable textile-based self-powered sensors, J. Mater. Chem. 4 (47) (2016) 18342–18353, https://doi.org/10.1039/c6ta08358g.
[27] K.K. Yeung, T. Huang, Y. Hua, K. Zhang, M.M.F. Yuen, Z. Gao, Recent advances in electrochemical sensors for wearable sweat monitoring: a review, IEEE Sensor. J. 21 (13) (2021) 14522–14539, https://doi.org/10.1109/jsen.2021.3074311.
[28] Q. Zhai, L.W. Yap, R. Wang, S. Gong, Z. Guo, Y. Liu, Q. Lyu, J. Wang, G.P. Simon, W. Cheng, Vertically aligned gold nanowires as stretchable and wearable epidermal ion-selective electrode for noninvasive multiplexed sweat analysis, Anal. Chem. 92 (6) (2020) 4647–4655, https://doi.org/10.1021/acs.analchem.0c00274.
[29] J.H. Yoon, S.M. Kim, Y. Eom, J.M. Koo, H.W. Cho, T.J. Lee, K.G. Lee, H.J. Park, Y.K. Kim, H.J. Yoo, S.Y. Hwang, J. Park, B.G. Choi, Extremely fast self-healable bio-based supramolecular polymer for wearable real-time sweat-monitoring sensor, ACS Appl. Mater. Interfaces 11 (49) (2019) 46165–46175, https://doi.org/10.1021/acsami.9b16829.
[30] M. Parrilla, M. Cuartero, S. Padrell Sanchez, M. Rajabi, N. Roxhed, F. Niklaus, G.A. Crespo, Wearable all-solid-state potentiometric microneedle patch for intradermal potassium detection, Anal. Chem. 91 (2) (2019) 1578–1586, https://doi.org/10.1021/acs.analchem.8b04877.
[31] C. Zhao, X. Li, Q. Wu, X. Liu, A thread-based wearable sweat nanobiosensor, Biosens. Bioelectron. 188 (2021) 113270, https://doi.org/10.1016/j.bios.2021.113270.
[32] G. Zhao, R. Liang, F. Wang, J. Ding, W. Qin, An all-solid-state potentiometric microelectrode for detection of copper in coastal sediment pore water, Sensor. Actuator. B Chem. 279 (2019) 369–373, https://doi.org/10.1016/j.snb.2018.09.125.
[33] T. Arakawa, K. Tomoto, H. Nitta, K. Toma, S. Takeuchi, T. Sekita, S. Minakuchi, K. Mitsubayashi, A wearable cellulose acetate-coated mouthguard biosensor for in vivo salivary glucose measurement, Anal. Chem. 92 (18) (2020) 12201–12207, https://doi.org/10.1021/acs.analchem.0c01201.
[34] L. Cao, G.C. Han, H. Xiao, Z. Chen, C. Fang, A novel 3D paper-based microfluidic electrochemical glucose biosensor based on rGO-TEPA/PB sensitive film, Anal. Chim. Acta 1096 (2020) 34–43, https://doi.org/10.1016/j.aca.2019.10.049.
[35] B. Wang, Y. Luo, L. Gao, B. Liu, G. Duan, High-performance field-effect transistor glucose biosensors based on bimetallic Ni/Cu metal-organic frameworks, Biosens. Bioelectron. 171 (2021) 112736, https://doi.org/10.1016/j.bios.2020.112736.
[36] T. Zhang, J. Ran, C. Ma, B. Yang, A universal approach to enhance glucose biosensor performance by building blocks of Au nanoparticles, Adv. Mater. Interfaces 7 (12) (2020) 2000227, https://doi.org/10.1002/admi.202000227.
[37] D.H. Keum, S.-K. Kim, J. Koo, G.-H. Lee, C. Jeon, J.W. Mok, B.H. Mun, K.J. Lee, E. Kamrani, C.-K. Joo, S. Shin, J.-Y. Sim, D. Myung, S.H. Yun, Z. Bao, S.K. Hahn, Wireless smart contact lens for diabetic diagnosis and therapy, Sci. Adv. 6 (17) (2020), eaba3252, https://doi.org/10.1126/sciadv.aba3252.
[38] Y. Jiang, T. Xia, L. Shen, J. Ma, H. Ma, T. Sun, F. Lv, N. Zhu, Facet-dependent Cu2O electrocatalysis for wearable enzyme-free smart sensing, ACS Catal. 11 (5) (2021) 2949–2955, https://doi.org/10.1021/acscatal.0c04797.
[39] R. Wang, Q. Zhai, T. An, S. Gong, W. Cheng, Stretchable gold fiber-based wearable textile electrochemical biosensor for lactate monitoring in sweat, Talanta 222 (2021) 121484, https://doi.org/10.1016/j.talanta.2020.121484.
[40] I. Shitanda, M. Mitsumoto, N. Loew, Y. Yoshihara, H. Watanabe, T. Mikawa, S. Tsujimura, M. Itagaki, M. Motosuke, Continuous sweat lactate monitoring system with integrated screen-printed MgO-templated carbon-lactate oxidase biosensor and microfluidic sweat collector, Electrochim. Acta 368 (2021) 137620, https://doi.org/10.1016/j.electacta.2020.137620.
[41] X. Wei, M. Zhu, J. Li, L. Liu, J. Yu, Z. Li, B. Ding, Wearable biosensor for sensitive detection of uric acid in artificial sweat enabled by a fiber structured sensing interface, Nano Energy 85 (2021) 106031, https://doi.org/10.1016/j.nanoen.2021.106031.
[42] R.M. Torrente-Rodriguez, J. Tu, Y. Yang, J. Min, M. Wang, Y. Song, Y. Yu, C. Xu, C. Ye, W.W. IsHak, W. Gao, Investigation of cortisol dynamics in human sweat using a graphene-based wireless mHealth system, Matter 2 (4) (2020) 921–937, https://doi.org/10.1016/j.matt.2020.01.021.
[43] D. Shanbhag, K. Bindu, A.R. Aarathy, M. Ramesh, M. Sreejesh, H.S. Nagaraja, Hydrothermally synthesized reduced graphene oxide and Sn doped manganese dioxide nanocomposites for supercapacitors and dopamine sensors, Mater. Today Energy 4 (2017) 66–74, https://doi.org/10.1016/j.mtener.2017.03.006.
[44] Q. Wang, Y. Liu, J.C. Campillo-Brocal, A. Jimenez-Quero, G.A. Crespo, M. Cuartero, Electrochemical biosensor for glycine detection in biological fluids, Biosens. Bioelectron. 182 (2021) 113154, https://doi.org/10.1016/j.bios.2021.113154.
[45] L.C. Tai, C.H. Ahn, H.Y.Y. Nyein, W. Ji, M. Bariya, Y. Lin, L. Li, A. Javey, Nicotine monitoring with a wearable sweat band, ACS Sens. 5 (6) (2020) 1831–1837, https://doi.org/10.1021/acssensors.0c00791.
[46] R.M. Cardoso, P.R.L. Silva, A.P. Lima, D.P. Rocha, T.C. Oliveira, T.M. do Prado, E. L. Fava, O. Fatibello-Filho, E.M. Richter, R.A.A. Muñoz, 3D-Printed graphene/polylactic acid electrode for bioanalysis: biosensing of glucose and simultaneous determination of uric acid and nitrite in biological fluids, Sensor. Actuator. B Chem. 307 (2020) 127621, https://doi.org/10.1016/j.snb.2019.127621.
[47] Q. Zhang, D. Jiang, C. Xu, Y. Ge, X. Liu, Q. Wei, L. Huang, X. Ren, C. Wang, Y. Wang, Wearable electrochemical biosensor based on molecularly imprinted Ag nanowires for noninvasive monitoring lactate in human sweat, Sensor. Actuator. B Chem. 320 (2020) 128325, https://doi.org/10.1016/j.snb.2020.128325.
[48] L. Durai, C.Y. Kong, S. Badhulika, One-step solvothermal synthesis of nanoflake-nanorod WS2 hybrid for non-enzymatic detection of uric acid and quercetin in blood serum, Mater. Sci. Eng. C Mater. Biol. Appl. 107 (2020) 110217, https://doi.org/10.1016/j.msec.2019.110217.
[49] Z. Khosroshahi, F. Karimzadeh, M. Kharaziha, A. Allafchian, A non-enzymatic sensor based on three-dimensional graphene foam decorated with Cu-xCu2O nanoparticles for electrochemical detection of glucose and its application in human serum, Mater. Sci. Eng. C Mater. Biol. Appl. 108 (2020) 110216, https://doi.org/10.1016/j.msec.2019.110216.
[50] S. Lin, B. Wang, W. Yu, K. Castillo, C. Hoffman, X. Cheng, Y. Zhao, Y. Gao, Z. Wang, H. Lin, H. Hojaiji, J. Tan, S. Emaminejad, Design framework and sensing system for noninvasive wearable electroactive drug monitoring, ACS Sens. 5 (1) (2020) 265–273, https://doi.org/10.1021/acssensors.9b02233.
[51] U. Farooq, M.W. Ullah, Q. Yang, A. Aziz, J. Xu, L. Zhou, S. Wang, High-density phage particles immobilization in surface-modified bacterial cellulose for

ultra-sensitive and selective electrochemical detection of Staphylococcus aureus, Biosens. Bioelectron. 157 (2020) 112163, https://doi.org/10.1016/j.bios.2020.112163.
[52] X. Du, Z. Zhang, X. Zheng, H. Zhang, D. Dong, Z. Zhang, M. Liu, J. Zhou, An electrochemical biosensor for the detection of epithelial-mesenchymal transition, Nat. Commun. 11 (1) (2020) 192, https://doi.org/10.1038/s41467-019-14037-w.
[53] M. Ku, J. Kim, J.-E. Won, W. Kang, Y.-G. Park, J. Park, J.-H. Lee, J. Cheon, H.H. Lee, J.-U. Park, Smart, soft contact lens for wireless immunosensing of cortisol, Sci. Adv. 6 (28) (2020), eabb2891, https://doi.org/10.1126/sciadv.abb2891.
[54] M. Foguel, G. Furlan Giordano, C. de Sylos, I. Carlos, A. Pupim Ferreira, A. Benedetti, H. Yamanaka, A low-cost label-free AFB1 impedimetric immunosensor based on functionalized CD-trodes, Chemosensors 4 (3) (2016) 7–10, https://doi.org/10.3390/chemosensors4030017.
[55] W. He, C. Wang, H. Wang, M. Jian, W. Lu, X. Liang, X. Zhang, F. Yang, Y. Zhang, Integrated textile sensor patch for real-time and multiplex sweat analysis, Sci. Adv. 5 (11) (2019), aax0649, https://doi.org/10.1126/sciadv.aax0649.
[56] X. He, S. Yang, Q. Pei, Y. Song, C. Liu, T. Xu, X. Zhang, Integrated smart janus textile bands for self-pumping sweat sampling and analysis, ACS Sens. 5 (6) (2020) 1548–1554, https://doi.org/10.1021/acssensors.0c00563.
[57] G. Xu, C. Cheng, Z. Liu, W. Yuan, X. Wu, Y. Lu, S.S. Low, J. Liu, L. Zhu, D. Ji, S. Li, Z. Chen, L. Wang, Q. Yang, Z. Cui, Q. Liu, Battery-free and wireless epidermal electrochemical system with all-printed stretchable electrode array for multiplexed in situ sweat analysis, Adv. Mater. Technol. 4 (7) (2019) 1800658, https://doi.org/10.1002/admt.201800658.
[58] E. Bakker, P. Buhlmann, E. Pretsch, Carrier-based ion-selective electrodes and bulk optodes. 1. General characteristics, Chem. Rev. 97 (8) (1997) 3083–3132, https://doi.org/10.1021/cr940394a.
[59] S. Emaminejad, W. Gao, E. Wu, Z.A. Davies, H.Y.Y. Nyein, S. Challa, S.P. Ryan, H.M. Fahad, K. Chen, Z. Shahpar, S. Talebi, C. Milla, A. Javey, R.W. Davis, Autonomous sweat extraction and analysis applied to cystic fibrosis and glucose monitoring using a fully integrated wearable platform, Proc. Natl. Acad. Sci. U. S. A 114 (18) (2017) 4625–4630, https://doi.org/10.1073/pnas.1701740114.
[60] S. Anastasova, B. Crewther, P. Bembnowicz, V. Curto, H.M.D. Ip, B. Rosa, G.-Z. Yang, A wearable multisensing patch for continuous sweat monitoring, Biosens. Bioelectron. 93 (2017) 139–145, https://doi.org/10.1016/j.bios.2016.09.038.
[61] J. Madden, C. O'Mahony, M. Thompson, A. O'Riordan, P. Galvin, Biosensing in dermal interstitial fluid using microneedle based electrochemical devices, Sens. Bio-Sens. Res. 29 (2020) 100348, https://doi.org/10.1016/j.sbsr.2020.100348.
[62] H. Lee, T.K. Choi, Y.B. Lee, H.R. Cho, R. Ghaffari, L. Wang, H.J. Choi, T.D. Chung, N. Lu, T. Hyeon, S.H. Choi, D.-H. Kim, A graphene-based electrochemical device with thermoresponsive microneedles for diabetes monitoring and therapy, Nat. Nanotechnol. 11 (6) (2016) 566–572, https://doi.org/10.1038/nnano.2016.38.
[63] E. Sohouli, E.M. Khosrowshahi, P. Radi, E. Naghian, M. Rahimi-Nasrabadi, F. Ahmadi, Electrochemical sensor based on modified methylcellulose by graphene oxide and Fe3O4 nanoparticles: application in the analysis of uric acid content in urine, J. Electroanal. Chem. 877 (2020) 114503, https://doi.org/10.1016/j.jelechem.2020.114503.
[64] Q. Zheng, Q. Tang, Z.L. Wang, Z. Li, Self-powered cardiovascular electronic devices and systems, Nat. Rev. Cardiol. 18 (1) (2021) 7–21, https://doi.org/10.1038/s41569-020-0426-4.
[65] H. Zhang, Y. Yang, T.-C. Hou, Y. Su, C. Hu, Z.L. Wang, Triboelectric nanogenerator built inside clothes for self-powered glucose biosensors, Nano Energy 2 (5) (2013) 1019–1024, https://doi.org/10.1016/j.nanoen.2013.03.024.
[66] T. Zhao, C. Zheng, H. He, H. Guan, T. Zhong, L. Xing, X. Xue, A self-powered biosensing electronic-skin for real-time sweat Ca2+ detection and wireless data transmission, Smart Mater. Struct. 28 (8) (2019), 085015, https://doi.org/10.1088/1361-665X/ab2624.
[67] Y. Kim, X. Wu, C. Lee, J.H. Oh, Characterization of PI/PVDF-TrFE composite nanofiber-based triboelectric nanogenerators depending on the type of the electrospinning system, ACS Appl. Mater. Interfaces 13 (31) (2021) 36967–36975, https://doi.org/10.1021/acsami.1c04450.
[68] J. Rao, Z. Chen, D. Zhao, R. Ma, W. Yi, C. Zhang, D. Liu, X. Chen, Y. Yang, X. Wang, J. Wang, Y. Yin, X. Wang, G. Yang, F. Yi, Tactile electronic skin to simultaneously detect and distinguish between temperature and pressure based on a triboelectric nanogenerator, Nano Energy 75 (2020) 105073, https://doi.org/10.1016/j.nanoen.2020.105073.
[69] Y. Yang, H. Pan, G. Xie, Y. Jiang, C. Chen, Y. Su, Y. Wang, H. Tai, Flexible piezoelectric pressure sensor based on polydopamine-modified BaTiO3/PVDF composite film for human motion monitoring, Sens. Actuator Phys. 301 (2020) 111789, https://doi.org/10.1016/j.sna.2019.111789.
[70] S. Yang, X. Cui, R. Guo, Z. Zhang, S. Sang, H. Zhang, Piezoelectric sensor based on graphene-doped PVDF nanofibers for sign language translation, Beilstein J. Nanotechnol. 11 (2020) 1655–1662, https://doi.org/10.3762/bjnano.11.148.
[71] K. Zhao, B. Ouyang, C.R. Bowen, Z.L. Wang, Y. Yang, One-structure-based multi-effects coupled nanogenerators for flexible and self-powered multi-functional coupled sensor systems, Nano Energy 71 (2020) 104632, https://doi.org/10.1016/j.nanoen.2020.104632.
[72] Y. Mao, W. Yue, T. Zhao, M. Shen, B. Liu, S. Chen, A self-powered biosensor for monitoring maximal lactate steady state in sport training, Biosens. Bioelectron. 10 (7) (2020) 75, https://doi.org/10.3390/bios10070075.
[73] J. Zhang, J. Liu, H. Su, F. Sun, Z. Lu, A. Su, A wearable self-powered biosensor system integrated with diaper for detecting the urine glucose of diabetic patients, Sensor. Actuator. B Chem. 341 (2021) 130046, https://doi.org/10.1016/j.snb.2021.130046.
[74] X. Li, Q. Feng, K. Lu, J. Huang, Y. Zhang, Y. Hou, H. Qiao, D. Li, Q. Wei, Encapsulating enzyme into metal-organic framework during in-situ growth on cellulose acetate nanofibers as self-powered glucose biosensor, Biosens. Bioelectron. 171 (2021) 112690, https://doi.org/10.1016/j.bios.2020.112690.
[75] Y. Yu, J. Nassar, C. Xu, J. Min, Y. Yang, A. Dai, R. Doshi, A. Huang, Y. Song, R. Gehlhar, A.D. Ames, W. Gao, Biofuel-powered soft electronic skin with multiplexed and wireless sensing for human-machine interfaces, Sci. Robotics 5 (41) (2020), eaaz7946, https://doi.org/10.1126/scirobotics.aaz7946.
[76] T. Sung, L. Shen, Y. Jiang, J. Ma, F. Lv, H. Ma, D. Chen, N. Zhu, Wearable textile supercapacitors for self-powered enzyme-free smartsensors, ACS Appl. Mater. Interfaces 12 (19) (2020) 21779–21787, https://doi.org/10.1021/acsami.0c05465.
[77] N. Zhang, F. Huang, S. Zhao, X. Lv, Y. Zhou, S. Xiang, S. Xu, Y. Li, G. Chen, C. Tao, Y. Nie, J. Chen, X. Fan, Photo-rechargeable fabrics as sustainable and robust power sources for wearable bioelectronics, Matter 2 (5) (2020) 1260–1269, https://doi.org/10.1016/j.matt.2020.01.022.
[78] J. Yuan, R. Zhu, G. Li, Self-powered electronic skin with multisensory functions based on thermoelectric conversion, Adv. Mater. Technol. 5 (9) (2020) 2000419, https://doi.org/10.1002/admt.202000419.
[79] K. Roy, S.K. Ghosh, A. Sultana, S. Garain, M. Xie, C.R. Bowen, K. Henkel, D. Schmeißer, D. Mandal, A self-powered wearable pressure sensor and pyroelectric breathing sensor based on GO interfaced PVDF nanofibers, ACS Appl. Nano Mater. 2 (4) (2019) 2013–2025, https://doi.org/10.1021/acsanm.9b00033.
[80] H. Guan, T. Zhong, H. He, T. Zhao, L. Xing, Y. Zhang, X. Xue, A self-powered wearable sweat-evaporation-biosensing analyzer for building sports big data, Nano Energy 59 (2019) 754–761, https://doi.org/10.1016/j.nanoen.2019.03.026.
[81] W. Zhang, H. Guan, T. Zhong, T. Zhao, L. Xing, X. Xue, Wearable battery-free perspiration analyzing sites based on sweat flowing on ZnO nanoarrays, Nano-Micro Lett. 12 (1) (2020) 105, https://doi.org/10.1007/s40820-020-00441-1.
[82] D. Shen, M. Xiao, G. Zou, L. Liu, W.W. Duley, Y.N. Zhou, Self-powered wearable electronics based on moisture enabled electricity generation, Adv. Mater. 30 (18) (2018) 1705925, https://doi.org/10.1002/adma.201705925.
[83] Z. Li, Q. Zheng, Z.L. Wang, Z. Li, Nanogenerator-based self-powered sensors for wearable and implantable electronics, Research (Washington, D.C.) 2020 (2020) 8710686, https://doi.org/10.34133/2020/8710686.
[84] L. Liu, X. Yang, L. Zhao, W. Xu, J. Wang, Q. Yang, Q. Tang, Nanowrinkle-patterned flexible woven triboelectric nanogenerator toward self-powered wearable electronics, Nano Energy 73 (2020) 104797, https://doi.org/10.1016/j.nanoen.2020.104797.
[85] T. Huang, J. Zhang, B. Yu, H. Yu, H. Long, H. Wang, Q. Zhang, M. Zhu, Fabric texture design for boosting the performance of a knitted washable textile triboelectric nanogenerator as wearable power, Nano Energy 58 (2019) 375–383, https://doi.org/10.1016/j.nanoen.2019.01.038.
[86] Z.L. Wang, Piezopotential gated nanowire devices: piezotronics and piezo-phototronics, Nano Today 5 (6) (2010) 540–552, https://doi.org/10.1016/j.nantod.2010.10.008.
[87] W. Wu, Z.L. Wang, Piezotronics and piezo-phototronics for adaptive electronics and optoelectronics, Nat. Rev. Mater. 1 (7) (2016) 16031, https://doi.org/10.1038/natrevmats.2016.31.
[88] M.-H. You, X.-X. Wang, X. Yan, J. Zhang, W.-Z. Song, M. Yu, Z.-Y. Fan, S. Ramakrishna, Y.-Z. Long, A self-powered flexible hybrid piezoelectric-pyroelectric nanogenerator based on non-woven nanofiber membranes, J. Mater. Chem. 6 (8) (2018) 3500–3509, https://doi.org/10.1039/c7ta10175a.
[89] X. Wang, W.-Z. Song, M.-H. You, J. Zhang, M. Yu, Z. Fan, S. Ramakrishna, Y.-Z. Long, Bionic single-electrode electronic skin unit based on piezoelectric nanogenerator, ACS Nano 12 (8) (2018) 8588–8596, https://doi.org/10.1021/acsnano.8b04244.
[90] S.K. Karan, S. Maiti, S. Paria, A. Maitra, S.K. Si, J.K. Kim, B.B. Khatua, A new insight towards eggshell membrane as high energy conversion efficient bio-piezoelectric energy harvester, Mater. Today Energy 9 (2018) 114–125, https://doi.org/10.1016/j.mtener.2018.05.006.
[91] P. Pinyou, V. Blay, L.M. Muresan, T. Noguer, Enzyme-modified electrodes for biosensors and biofuel cells, Mater. Horiz. 6 (7) (2019) 1336–1358, https://doi.org/10.1039/c9mh00013e.
[92] A. Polman, M. Knight, E.C. Garnett, B. Ehrler, W.C. Sinke, Photovoltaic materials: present efficiencies and future challenges, Science 352 (6283) (2016) aad4424, https://doi.org/10.1126/science.aad4424.
[93] Z. Wen, M.-H. Yeh, H. Guo, J. Wang, Y. Zi, W. Xu, J. Deng, L. Zhu, X. Wang, C. Hu, L. Zhu, X. Sun, Z.L. Wang, Self-powered textile for wearable electronics by hybridizing fiber-shaped nanogenerators, solar cells, and supercapacitors, Sci. Adv. 2 (10) (2016), e1600097, https://doi.org/10.1126/sciadv.1600097.
[94] Y. Lin, J. Chen, M.M. Tavakoli, Y. Gao, Y. Zhu, D. Zhang, M. Kam, Z. He, Z. Fan, Printable fabrication of a fully integrated and self-powered sensor system on

plastic substrates, Adv. Mater. 31 (5) (2019) 1804285, https://doi.org/10.1002/adma.201804285.
[95] A.S. Dahiya, J. Thireau, J. Boudaden, S. Lal, U. Gulzar, Y. Zhang, T. Gil, N. Azemard, P. Ramm, T. Kiessling, C. O'Murchu, F. Sebelius, J. Tilly, C. Glynn, S. Geary, C. O'Dwyer, K.M. Razeeb, A. Lacampagne, B. Charlot, A. Todri-Sanial, Review—energy autonomous wearable sensors for smart healthcare: a review, J. Electrochem. Soc. 167 (3) (2020), 037516, https://doi.org/10.1149/2.0162003jes.
[96] G. Rong, Y. Zheng, M. Sawan, Energy solutions for wearable sensors: a review, Sensors (Basel) 21 (11) (2021) 3806, https://doi.org/10.3390/s21113806.
[97] M. Wu, K. Yao, D. Li, X. Huang, Y. Liu, L. Wang, E. Song, J. Yu, X. Yu, Self-powered skin electronics for energy harvesting and healthcare monitoring, Materials Today Energy 21 (2021) 100786, https://doi.org/10.1016/j.mtener.2021.100786.
[98] D. Zhang, Y. Wang, Y. Yang, Design, performance, and application of thermoelectric nanogenerators, Small 15 (32) (2019), e1805241, https://doi.org/10.1002/smll.201805241.
[99] E. Liu, A. Negm, M.M.R. Howlader, Thermoelectric generation via tellurene for wearable applications: recent advances, research challenges, and future perspectives, Mater.Today Energy 20 (2021) 100625, https://doi.org/10.1016/j.mtener.2020.100625.
[100] H.A. Eivari, Z. Sohbatzadeh, P. Mele, M.H.N. Assadi, Low thermal conductivity: fundamentals and theoretical aspects in thermoelectric applications, Mater. Today Energy 21 (2021) 100744, https://doi.org/10.1016/j.mtener.2021.100744.
[101] Y. Yang, W. Guo, K.C. Pradel, G. Zhu, Y. Zhou, Y. Zhang, Y. Hu, L. Lin, Z.L. Wang, Pyroelectric nanogenerators for harvesting thermoelectric energy, Nano Lett. 12 (6) (2012) 2833–2838, https://doi.org/10.1021/nl3003039.
[102] L. Niu, F. Liu, Q. Zeng, X. Zhu, Y. Wang, P. Yu, J. Shi, J. Lin, J. Zhou, Q. Fu, W. Zhou, T. Yu, X. Liu, Z. Liu, Controlled synthesis and room-temperature pyroelectricity of CuInP2S6 ultrathin flakes, Nano Energy 58 (2019) 596–603, https://doi.org/10.1016/j.nanoen.2019.01.085.
[103] X. Dong, Z. Shi, C. Xu, C. Yang, F. Chen, M. Lei, J. Wang, Q. Cui, CdS quantum dots/Au nanoparticles/ZnO nanowire array for self-powered photoelectrochemical detection of Escherichia coli O157:H7, Biosens. Bioelectron. 149 (2020) 111843, https://doi.org/10.1016/j.bios.2019.111843.
[105] W.-Z. Song, X.-X. Wang, H.-J. Qiu, Q. Liu, J. Zhang, Z. Fan, M. Yu, S. Ramakrishna, H. Hu, Y.-Z. Long, Sliding non-contact inductive nanogenerator, Nano Energy 63 (2019) 103878, https://doi.org/10.1016/j.nanoen.2019.103878.
[106] D.Y. Park, D.J. Joe, D.H. Kim, H. Park, J.H. Han, C.K. Jeong, H. Park, J.G. Park, B. Joung, K.J. Lee, Self-powered real-time arterial pulse monitoring using ultrathin epidermal piezoelectric sensors, Adv. Mater. 29 (37) (2017) 1702308, https://doi.org/10.1002/adma.201702308.
[107] Z. Lin, J. Chen, X. Li, Z. Zhou, K. Meng, W. Wei, J. Yang, Z.L. Wang, Triboelectric nanogenerator enabled body sensor network for self-powered human heart-rate monitoring, ACS Nano 11 (9) (2017) 8830–8837, https://doi.org/10.1021/acsnano.7b02975.
[108] H. He, H. Zeng, Y. Fu, W. Han, Y. Dai, L. Xing, Y. Zhang, X. Xue, A self-powered electronic-skin for real-time perspiration analysis and application in motion state monitoring, J. Mater. Chem. C 6 (36) (2018) 9624–9630, https://doi.org/10.1039/c8tc03296c.
[109] G. Slaughter, T. Kulkarni, Highly selective and sensitive self-powered glucose sensor based on capacitor circuit, Sci. Rep. 7 (1) (2017) 1471, https://doi.org/10.1038/s41598-017-01665-9.
[110] A.J. Bandodkar, J.-M. You, N.-H. Kim, Y. Gu, R. Kumar, A.M.V. Mohan, J. Kurniawan, S. Imani, T. Nakagawa, B. Parish, M. Parthasarathy, P.P. Mercier, S. Xu, J. Wang, Soft, stretchable, high power density electronic skin-based biofuel cells for scavenging energy from human sweat, Energy Environ. Sci. 10 (7) (2017) 1581–1589, https://doi.org/10.1039/c7ee00865a.
[111] Y. Yang, S. Wang, Y. Zhang, Z.L. Wang, Pyroelectric nanogenerators for driving wireless sensors, Nano Lett. 12 (12) (2012) 6408–6413, https://doi.org/10.1021/nl303755m.
[112] J. Yuan, R. Zhu, A fully self-powered wearable monitoring system with systematically optimized flexible thermoelectric generator, Appl. Energy 271 (2020) 115250, https://doi.org/10.1016/j.apenergy.2020.115250.
[113] W. Harmon, D. Bamgboje, H. Guo, T. Hu, Z.L. Wang, Self-driven power management system for triboelectric nanogenerators, Nano Energy 71 (2020) 104642, https://doi.org/10.1016/j.nanoen.2020.104642.
[114] A. Ghaffarinejad, J.Y. Hasani, R. Hinchet, Y. Lu, H. Zhang, A. Karami, D. Galayko, S.-W. Kim, P. Basset, A conditioning circuit with exponential enhancement of output energy for triboelectric nanogenerator, Nano Energy 51 (2018) 173–184, https://doi.org/10.1016/j.nanoen.2018.06.034.
[115] C. Zhang, J. Chen, W. Xuan, S. Huang, B. You, W. Li, L. Sun, H. Jin, X. Wang, S. Dong, J. Luo, A.J. Flewitt, Z.L. Wang, Conjunction of triboelectric nanogenerator with induction coils as wireless power sources and self-powered wireless sensors, Nat. Commun. 11 (1) (2020) 58, https://doi.org/10.1038/s41467-019-13653-w.
[116] X. Cheng, L. Miao, Y. Song, Z. Su, H. Chen, X. Chen, J. Zhang, H. Zhang, High efficiency power management and charge boosting strategy for a triboelectric nanogenerator, Nano Energy 38 (2017) 438–446, https://doi.org/10.1016/j.nanoen.2017.05.063.
[117] X. Xia, H. Wang, P. Basset, Y. Zhu, Y. Zi, Inductor-free output multiplier for power promotion and management of triboelectric nanogenerators toward self-powered systems, ACS Appl. Mater. Interfaces 12 (5) (2020) 5892–5900, https://doi.org/10.1021/acsami.9b20060.
[118] H. Chen, Y. Song, X. Cheng, H. Zhang, Self-powered electronic skin based on the triboelectric generator, Nano Energy 56 (2019) 252–268, https://doi.org/10.1016/j.nanoen.2018.11.061.
[119] S. Lu, L. Gao, X. Chen, D. Tong, W. Lei, P. Yuan, X. Mu, H. Yu, Simultaneous energy harvesting and signal sensing from a single triboelectric nanogenerator for intelligent self-powered wireless sensing systems, Nano Energy 75 (2020) 104813, https://doi.org/10.1016/j.nanoen.2020.104813.
[120] S. Niu, X. Wang, F. Yi, Y.S. Zhou, Z.L. Wang, A universal self-charging system driven by random biomechanical energy for sustainable operation of mobile electronics, Nat. Commun. 6 (2015) 8975, https://doi.org/10.1038/ncomms9975.
[121] X. Pu, L. Li, H. Song, C. Du, Z. Zhao, C. Jiang, G. Cao, W. Hu, Z.L. Wang, A self-charging power unit by integration of a textile triboelectric nanogenerator and a flexible lithium-ion battery for wearable electronics, Adv. Mater. 27 (15) (2015) 2472–2478, https://doi.org/10.1002/adma.201500311.
[122] Q. Zhang, Q. Liang, Q. Liao, M. Ma, F. Gao, X. Zhao, Y. Song, L. Song, X. Xun, Y. Zhang, An amphiphobic hydraulic triboelectric nanogenerator for a self-cleaning and self-charging power system, Adv. Funct. Mater. 28 (35) (2018) 1803117, https://doi.org/10.1002/adfm.201803117.
[123] X. Hou, J. Zhu, J. Qian, X. Niu, J. He, J. Mu, W. Geng, C. Xue, X. Chou, Stretchable triboelectric textile composed of wavy conductive-cloth PET and patterned stretchable electrode for harvesting multivariant human motion energy, ACS Appl. Mater. Interfaces 10 (50) (2018) 43661–43668, https://doi.org/10.1021/acsami.8b16267.
[124] W. Tang, C. Zhang, C.B. Han, Z.L. Wang, Enhancing output power of cylindrical triboelectric nanogenerators by segmentation design and multilayer integration, Adv. Funct. Mater. 24 (42) (2014) 6684–6690, https://doi.org/10.1002/adfm.201401936.
[125] G. Zhu, J. Chen, T. Zhang, Q. Jing, Z.L. Wang, Radial-arrayed rotary electrification for high performance triboelectric generator, Nat. Commun. 5 (2014) 3426, https://doi.org/10.1038/ncomms4426.
[126] F. Xi, Y. Pang, W. Li, T. Jiang, L. Zhang, T. Guo, G. Liu, C. Zhang, Z.L. Wang, Universal power management strategy for triboelectric nanogenerator, Nano Energy 37 (2017) 168–176, https://doi.org/10.1016/j.nanoen.2017.05.027.
[127] W. Harmon, D. Bamgboje, H.Y. Guo, T.S. Hu, Z.L. Wang, Self-driven power management system for triboelectric nanogenerators, Nano Energy 71 (2020) 104642, https://doi.org/10.1016/j.nanoen.2020.104642.
[128] K. Meng, J. Chen, X. Li, Y. Wu, W. Fan, Z. Zhou, Q. He, X. Wang, X. Fan, Y. Zhang, J. Yang, Z.L. Wang, Flexible weaving constructed self-powered pressure sensor enabling continuous diagnosis of cardiovascular disease and measurement of cuffless blood pressure, Adv. Funct. Mater. (2018), https://doi.org/10.1002/adfm.201806388.
[129] X.H. Li, Z.H. Lin, G. Cheng, X.N. Wen, Y. Liu, S.M. Niu, Z.L. Wang, 3D fiber-based hybrid nanogenerator for energy harvesting and as a self-powered pressure sensor, ACS Nano 8 (10) (2014) 10674–10681, https://doi.org/10.1021/nn504243j.
[130] M. Pan, C. Yuan, X. Liang, J. Zou, Y. Zhang, C. Bowen, Triboelectric and piezoelectric nanogenerators for future soft robots and machines, iScience 23 (11) (2020) 101682, https://doi.org/10.1016/j.isci.2020.101682.
[131] A.A. Khan, A. Mahmud, D. Ban, Evolution from single to hybrid nanogenerator: a contemporary review on multimode energy harvesting for self-powered electronics, IEEE Trans. Nanotechnol. 18 (2019) 21–36, https://doi.org/10.1109/tnano.2018.2876824.
[132] Z. Wu, T. Cheng, Z.L. Wang, Self-powered sensors and systems based on nanogenerators, Sensors (Basel) 20 (10) (2020) 2925, https://doi.org/10.3390/s20102925.
[133] Q. Shi, Z. Sun, Z. Zhang, C. Lee, Triboelectric nanogenerators and hybridized systems for enabling next-generation IoT applications, Research (Wash D C) 2021 (2021) 6849171, https://doi.org/10.34133/2021/6849171.
[134] W.S. Jung, M.G. Kang, H.G. Moon, S.H. Baek, S.J. Yoon, Z.L. Wang, S.W. Kim, C.Y. Kang, High output piezo/triboelectric hybrid generator, Sci. Rep. 5 (2015) 9309, https://doi.org/10.1038/srep09309.
[135] T. Kulkarni, G. Slaughter, Characteristics of two self-powered glucose biosensors, IEEE Sensor. J. 17 (12) (2017) 3607–3612, https://doi.org/10.1109/jsen.2017.2696260.
[136] S. Hao, X. Sun, H. Zhang, J. Zhai, S. Dong, Recent development of biofuel cell based self-powered biosensors, J. Mater. Chem. B 8 (16) (2020) 3393–3407, https://doi.org/10.1039/c9tb02428j.
[137] E. Cho, M. Mohammadifar, S. Choi, A single-use, self-powered, paper-based sensor patch for detection of exercise-induced hypoglycemia, Micromachines (Basel) 8 (9) (2017) 265, https://doi.org/10.3390/mi8090265.
[138] S. Hao, H. Zhang, X. Sun, J. Zhai, S. Dong, A mediator-free self-powered glucose biosensor based on a hybrid glucose/MnO2 enzymatic biofuel cell, Nano Res. 14 (3) (2020) 707–714, https://doi.org/10.1007/s12274-020-3101-5.
[139] A.F. Yeknami, X. Wang, I. Jeerapan, S. Imani, A. Nikoofard, J. Wang, P.P. Mercier, A 0.3-V CMOS biofuel-cell-powered wireless glucose/lactate biosensing system, IEEE J. Solid State Circ. 53 (11) (2018) 3126–3139, https://doi.org/10.1109/jssc.2018.2869569.
[140] A.F. Yeknami, X.Y. Wang, S. Imani, A. Nikoofard, I. Jeerapan, J. Wang, P.P. Mercier, A 0.3V biofuel-cell-powered glucose/lactate biosensing system employing a 180nW 64dB SNR passive delta sigma ADC and a 920MHz

wireless transmitter, ISSCC Dig. Tech. Pap. I (2018) 284–286, https://doi.org/10.1109/ISSCC.2018.8310295.
[141] A. DeHennis, S. Getzlaff, D. Grice, M. Mailand, An NFC-enabled CMOS IC for a wireless fully implantable glucose sensor, IEEE J. Biomed. Health Inform. 20 (1) (2016) 18–28, https://doi.org/10.1109/JBHI.2015.2475236.
[142] A.F. Yeknami, X. Wang, S. Imani, A. Nikoofard, I. Jeerapan, J. Wang, P.P. Mercier, A 0.3V biofuel-cell-powered glucose/lactate biosensing system employing a 180nW 64dB SNR passive δς ADC and a 920MHz wireless transmitter, in: 2018 IEEE International Solid - State Circuits Conference - (ISSCC), 2018, pp. 284–286, https://doi.org/10.1109/ISSCC.2018.8310295.
[143] M. Dei, J. Aymerich, M. Piotto, P. Bruschi, F. del Campo, F. Serra-Graells, CMOS interfaces for internet-of-wearables electrochemical sensors: trends and challenges, Electronics 8 (2) (2019) 150, https://doi.org/10.3390/electronics8020150.
[144] D.P. Rose, M.E. Ratterman, D.K. Griffin, L. Hou, N. Kelley-Loughnane, R.R. Naik, J.A. Hagen, I. Papautsky, J.C. Heikenfeld, Adhesive RFID sensor patch for monitoring of sweat electrolytes, IEEE Trans. Biomed. Eng. 62 (6) (2015) 1457–1465, https://doi.org/10.1109/TBME.2014.2369991.
[145] P. Kassal, M.D. Steinberg, I.M. Steinberg, Wireless chemical sensors and biosensors: a review, Sensor. Actuator. B Chem. 266 (2018) 228–245, https://doi.org/10.1016/j.snb.2018.03.074.